Using Hydrogeomorphic Features to Quantify Structural and Functional Hydrologic Connectivity in a Coastal Plain Headwater Stream

Delaney M. Peterson[1], C. Nathan Jones[1], Alain M. Plattner[2], Arial J. Shogren[1], and Sarah E. Godsey[3]

[1]Department of Biological Sciences, University of Alabama, Tuscaloosa, AL, USA.

[2]Department of Geological Sciences, University of Alabama, Tuscaloosa, AL, USA.

[3]Department of Geosciences, Idaho State University, Pocatello, ID, USA.

Corresponding author: Delaney Peterson (dmpeterson2@crimson.edu)

Author ORCIDs:

Peterson: 0000-0002-3444-4772

Jones: 0000-0002-5804-0510

Plattner: 0000-0001-5154-1833

Shogren: 0000-0002-1284-3836

Godsey: 0000-0001-6529-7886

This is a non-peer-reviewed manuscript being submitted to Water Resources Research.

Key Points:

- Hydrogeomorphic features provide a key framework to study streamflow generation along the river corridor.
- Across the study watershed, hydrogeomorphic features demonstrated distinct patterns of groundwater-surface water connectivity.
- Within hydrogeomorphic features, spatial variability in clay confining layers led to temporal variability in perched flowpath activation.

Abstract

Headwater streams comprise most of the global river length, and hydrologic processes occurring in headwaters affect the chemical, physical, and biological functions of downstream aquatic ecosystems. However, we do not have a clear understanding of the spatial scales that drive hydrologic processes across headwater systems, particularly in Coastal Plain landscapes. We address this gap by characterizing hydrologic connectivity in a small, forested watershed in the Coastal Plain of Alabama, USA. We collected data across three spatial scales: the watershed (0.9 km^2), hydrogeomorphic feature (100-500 m), and hillslope (10-100 m) scales. We characterized stream network variability using seasonal surveys combined with water monitoring wells to characterize stream hydrologic state across 2021, paired with an Electrical Resistivity Tomography (ERT) and Time Domain Induced Polarization (TDIP) survey to characterize subsurface structure. Our results suggest that discretizing the river corridor into distinct hydrogeomorphic features provides a framework for understanding the dynamics of hydrologic connectivity within a watershed. Each hydrogeomorphic feature experienced consistent hydrologic states that differed along the network: incised channels gained water, intact riparian zones lost water, and wetland-stream complexes reflected no net water gain or loss from the river corridor. Subsurface structures observed with the ERT/TDIP survey indicate heterogeneous perched flowpaths, with saturation occurring variably throughout both space and time. Altogether, these results suggest that studying watersheds across a hierarchy of scales can reveal the dynamics of hydrologic connectivity, and that hydrogeomorphic features can provide a key intermediate scale for the integration of hydrologic processes across the river corridor.

Plain Language Summary

Small streams are vitally important water resources; they provide flood protection, important habitat for amphibians and fish, and often drinking water for downstream communities. However, small streams are highly variable, and this variability has limited our ability to reliably predict how small streams impact downstream areas across all landscapes. We address this knowledge gap by quantifying hydrologic connectivity – or the water-mediated movement of materials, energy, and organisms – across a watershed located in the southeastern US. We collected data across three spatial scales: the largest watershed scale (0.9 km^2), the intermediate scale that we define as the hydrogeomorphic feature scale (100-500 m), and the smallest hillslope scale (10-100 m). Our data suggest that splitting watersheds into separate hydrogeomorphic features that are defined by the shape of their valley provides a framework for understanding hydrologic connectivity in small streams. As an example, we found incised streams typically received water from surrounding hillslopes, whereas streams without incision typically lost water to the surrounding hillslope. Additionally, subsurface imaging suggests that patchy clay soils play an important role in the movement of water. Together, these results suggest that studying watershed across scales can help us understand how small streams impact downstream areas.

1 Introduction

Headwater streams comprise over 80% of global river networks (Downing et al., 2012), and are defined as low-order (i.e., 1st-3rd Strahler order, Golden et al., 2025; Vannote et al., 1980) streams that occupy the upper reaches of stream networks (Nadeau & Rains, 2007). Headwaters are important hydrologic features with unique physical (Alexander et al., 2007; Allen et al., 2018), chemical (Alexander et al., 2007; Peterson et al., 2001), and biological (Meyer et al., 2007; Richardson & Danehy, 2007) downstream impacts, and represent the dynamic interface between terrestrial hillslopes and aquatic ecosystems (Gomi et al., 2002; Lowe & Likens, 2005). However, most studies have focused on headwaters as low-order perennial streams mapped at the 1:100,000 scale (Doyle & Ensign, 2009; Nadeau & Rains, 2007), which often excludes the field-observable but difficult-to-map non-perennial and zero-order streams that feed downstream, mapped headwaters (Gomi et al., 2002; Shanafield et al., 2021). In many humid systems, most non-perennial stream reaches are found in the headwaters of stream networks (Costigan et al., 2016; Nadeau & Rains, 2007; Shanafield et al., 2021). Therefore, headwater systems are typically conceptualized such that perennial flow occurs where the permanent water table intersects with the hillslope, and channels upstream of this point only flow when seasonal or event-driven water table fluctuations intersect (Dunne & Black, 1970; Hewlett & Hibbert, 1967; Winter, 1999; Zimmer & McGlynn, 2017; Mahoney et al., 2023; Zanetti et al., 2024; Brinkerhoff et al., 2024).

Heterogeneity in the subsurface influences spatial and temporal patterns in streamflow in headwater systems (Klaus & Jackson 2018; Jackson et al. 2014; Zimmer & McGlynn 2017; Dohman et al. 2021). Preferential flow, or non-equilibrium flow, is the process by which infiltrating water and solutes are channelized into a small fraction of the available pore space in the subsurface (Jarvis et al., 2016). Perched flowpaths are a form of preferential flow that are driven by confining layers and soil horizons with contrasting hydraulic conductivities (Baird & Low, 2022; Nimmo, 2012; Weyman, 1973), and can lead to heterogeneity in subsurface saturation (e.g., shallow, transient, perched water tables; Zimmer & McGlynn, 2017). This heterogeneity in subsurface saturation can further result in source areas of streamflow that are variable across both space and time (Klaus & Jackson, 2018; Kirker & Toran, 2023). Along non-perennial reaches (i.e., areas upstream of where the permanent water table intersects with the surface; Busch et al., 2020), variability in source areas leads to variable patterns of wetting and drying along the channel (Zimmer & McGlynn, 2017). Thus, subsurface heterogeneity and the resulting perched, transient flowpaths can play an important role in patterns of network connectivity and disconnectivity (Klaus & Jackson, 2018; Jackson et al., 2014, Zimmer & McGlynn 2017; McGuire et al., 2024).

Hydrologic variability and streamflow generation are controlled by hierarchical drivers, or drivers that influence patterns at distinct spatial scales, and altogether interact in a predictable order when integrating across scales (*sensu* Jencso & McGlynn, 2011; Frissell et al., 1986; Poff, 1997). One of the foundational conceptualizations of the hierarchical drivers of flow in headwater streams is the Variable Source Area concept (Hewlett & Hibbert, 1967). This defined the drivers of network expansion and contraction in small humid-climate watersheds as primarily depth to impervious layers and similar soil characteristics, followed by watershed slope and topographic characteristics, then climatic factors like the magnitude and frequency of storm events, and lastly land use (Hewlett & Hibbert, 1967). Others have built upon this conceptualization by studying hydrologic processes across spatial scales from the soil grain, plot, reach, to watershed, and have found that watershed physiographic variables (i.e., geology, topography, soil structure) and land use also emerge as drivers of streamflow generation (Costigan et al., 2016; Jencso et al., 2009; McGuire et al., 2005; Prancevic & Kirchner, 2019; Spence, 2010; Trancoso et al., 2017; Warix et al., 2023). However, there are challenges to integrating across spatial scales to better understand hierarchical drivers and hydrologic processes. For example, spatial heterogeneity and threshold behavior span gradients of time and space, such that data collected at smaller scales might not represent the larger patterns that emerge within an entire watershed (emergent properties; Jencso et al., 2009; McDonnell et al., 2007). Further, streamflow generation processes do not easily organize into measurable scales, but rather integrate across all subordinate scales with respect to connectivity and heterogeneity, resulting in watersheds responding differently over time to the same factors and inputs (Spence, 2010). Therefore, it is difficult to predict how, when, and where these well-documented hierarchical drivers interact across scales to influence streamflow generation, and we are still looking for effective scales and methods of study to understand the shifting hierarchy of processes that drive the emergent properties of streamflow generation.

Hydrologic connectivity represents a conceptual framework that has the potential to unify concepts from across disciplines and spatial scales (Jones et al., 2019). Hydrologic connectivity is broadly defined as the water-mediated movement of materials, organisms, and energy between watershed components (Pringle, 2001; Rinderer et al., 2018), and provides a unifying concept that can be used to integrate the importance of water fluxes across disciplines (i.e., ecology, biogeochemistry, geomorphology, and hydrology; Jones et al., 2019; Larsen et al., 2012). Hydrologic connectivity is often measured as the magnitude, frequency, duration, and intensity of hydrologic exchange flows (Covino, 2017; Harvey & Gooseff, 2015), often across three spatial dimensions (vertical, lateral, and longitudinal) and time (Ward, 1989; Zimmer & McGlynn, 2018). Hydrologic connectivity can also be conceptualized through the lens of structural and functional connectivity (Bracken et al., 2013). Here, structural connectivity is the physical adjacency of watershed components that would allow connectivity. Functional connectivity is the resulting flux of water, solutes, and organisms (Larsen et al., 2012; Rinderer et al., 2018). However, while connectivity has been highly operationalized, the hydrologic science community has not adopted a universal measure or metric of connectivity that can be applied across sites and scales. Moreover there has been no uniform dimension or scale of connectivity that has been employed across all systems.

Across the hydrologic sciences, there are multiple research frameworks and associated communities of researchers working to understand streamflow generation; here, we will focus on hydrogeomorphology, river corridor science, and network dynamics research. Despite these three frameworks' aligned goals, they focus on different and distinct spatiotemporal scales. Hydrogeomorphology has been loosely defined as an interdisciplinary research area focused on the complex interactions between geomorphology and hydrology to understand aquatic ecosystems (Poole, 2010; Sidle & Onda, 2004). Therefore, hydrogeomorphology generally combines geomorphic principles (e.g., sediment regimes and channel bedform dynamics) with hydrologic principles (e.g., hydrologic fluxes and stream network dynamics) to characterize the physical template of systems. Alternatively, river corridor science is a recently defined area of study focused on hydrologic connectivity and riparian-stream corridor processes (Harvey & Gooseff, 2015). While initially focused on near-stream exchange flows at scales smaller than river reaches (e.g., geomorphic bedforms, Cardenas et al., 2004), river corridor science also aims to understand how hillslope and upland processes influence exchange flows in the river corridor (Harvey & Gooseff, 2015; Wymore et al., 2023). Finally, the network dynamics research community has recently focused on using stochastic network modeling to understand the patterns and processes of stream network expansion, contraction, connection, and disconnection (e.g., Aho et al., 2023; Botter & Durighetto, 2020; Prancevic & Kirchner, 2019). These studies utilize a perceptual model of hierarchical and stable drivers of wetting or drying at points within the network to investigate the potential drivers of connectivity dynamics at the network scale.

The spatial scales of the river corridor science, network dynamics, and hydrogeomorphology research frameworks are poorly aligned. River corridor science has focused on either patterns at the largest scales (10^4 to 10^7 m, Wymore et al., 2023) or processes at the smallest scales (sub-10 m, Harvey & Gooseff, 2015). Network dynamics research has focused on temporal snapshots of patterns at the watershed scale of 1-10 km^2 (e.g., Botter & Durighetto, 2020; Prancevic & Kirchner, 2019). Hydrogeomorphic research has focused on primarily reach and network scales (100 to 10^{10} m, Grabowski & Gurnell, 2016; Poole, 2010).

This intermediate scale allows for the study of both nested hydrologic processes and emergent properties, but is primarily focused on the channel itself. Therefore, we propose that hydrogeomorphic features – a functional unit on the order of 100 to 500 m that spans from the stream channel to the adjacent hillslope and integrates across compartments of the river corridor – should be used as the critical intermediate scale to study river corridor processes across the hydrogeomorphic continuum.

The Coastal Plain represents a largely understudied region, despite comprising over 1.1 million km^2 (>14%) of the continental US and representing a low-gradient system with diverse hierarchical drivers of streamflow generation. The Coastal Plain presents a unique physical template that will inform our understanding of how water moves through landscapes and challenge existing geographically-derived paradigms for high-gradient systems (Burt & McDonnell, 2015). Generally, landscapes organize into erosion-, transport-, and deposition-dominated zones based on topographic gradients (Jaeger et al., 2017; Schumm, 1977). However, due to the relatively lower topographic gradients in the Coastal Plain, variability in these zones can occur at surprisingly small scales (on the order of 1,000 m; Davis, 2007), emphasizing the need for an intermediate scale of study. Additionally, dominant processes in these zones can be strongly affected by the land-use legacies that dominate the landscape; in the southeastern USA specifically, land management decisions have resulted in consequences for forest community composition, soil structure, and stream channel structure and incision (Foster et al., 2003; Galang et al., 2007; Maloney et al., 2008). Further, in the low-gradient Coastal Plain and Piedmont of the southeastern USA, agricultural land-use legacies have resulted in severe erosion through both channel incision and gully formation (Trimble, 2008), which have documented effects on water table depth and subsurface storage (Hardison et al., 2009; Chen et al., 2020). While recent hydrology research has expanded into other low-gradient systems (e.g., Tetzlaff et al., 2011; Zimmer & McGlynn, 2017), and coastal alluvial plains (e.g., Epps et al., 2013; Lee et al., 2023), this physiographic province represents a key region where more work is needed.

In this study, we quantify hydrologic connectivity across spatial scales to elucidate drivers of streamflow generation in a low-gradient, Coastal Plain headwater system. We seek to: (i) identify an intermediate spatial scale (here, hydrogeomorphic features) that would allow us to integrate our understanding of structural connectivity across the entire river corridor; (ii) examine differences in hydrologic connectivity across hydrogeomorphic features in our study watershed; and (iii) document within-hydrogeomorphic feature heterogeneity using differences in structural and functional connectivity across the river corridor in our study watershed.

2 Materials and Methods

Our study characterizes hydrologic connectivity across three distinct spatial scales in a Coastal Plain headwater stream over the span of one calendar year (2021). At the coarsest watershed scale, we characterized hydrologic connectivity using geospatial data and seasonal stream network surveys to identify the active surface drainage network (ASDN). At the intermediate hydrogeomorphic feature scale, we characterized hydrologic connectivity using a combination of geospatial analysis and network of groundwater and surface water monitoring wells. Finally, at the finest hillslope scale, we characterized hydrologic connectivity using soil surveys, nested groundwater monitoring wells, and geophysical measurements.

2.1 Site Description

We conducted this study in a 0.9 km^2 low-gradient watershed located at the Tanglewood Biological Station in Hale County, AL (USA, Figure 1) from January 1 to December 31, 2021. The region has a humid subtropical climate and receives an average of 1,390 mm of precipitation per year as almost entirely rainfall (NOAA National Centers for Environmental information, 2023). In 2021, the annual precipitation was slightly above average with the area receiving 1,470 mm, 50% of which fell between June and September. The region has a mean annual temperature of 17.6°C, and the watershed-aggregated mean annual evapotranspiration is 986 mm (Running et al., 2021).

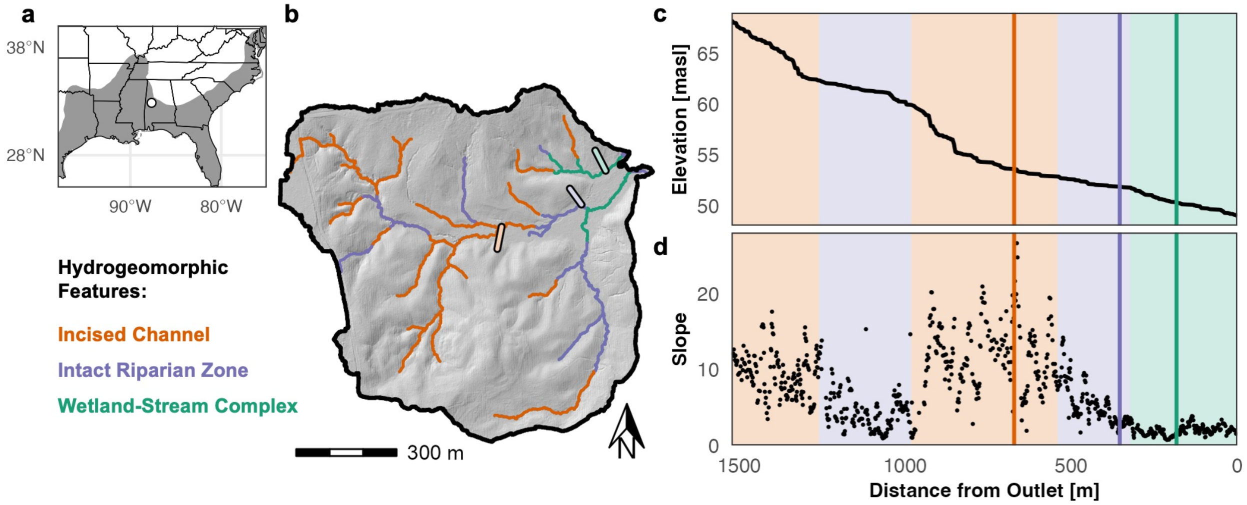

Figure 1. (**a**) A map of the southeastern US, with the Coastal Plain physiographic province highlighted in grey and the Tanglewood Biological Station indicated with a white point. (**b**) The 0.9 km^2 study watershed at the Tanglewood Biological Station, with elevation gradients shown as hillshade, and the stream network delineated by the solid line and colored according to hydrogeomorphic feature. These colors are used throughout all panels. The groundwater well transects are shown as segments perpendicular to the stream network. These transects also correspond to the well locations within the valley cross-sections in Figure 2. Additionally, one ERT/TDIP transect was performed along the well transect in the wetland-stream complex hydrogeomorphic feature. (**c**) A longitudinal profile of elevation of the streambed across the main channel of the stream network, colored by hydrogeomorphic features shown in (b). Additionally, locations of the well transects are marked by the solid vertical lines. (**d**) A longitudinal profile of stream channel slope across the main channel of the stream network and well transects are denoted by solid vertical lines, all colored by hydrogeomorphic features shown in (b).

Physiographically, this site is in the Coastal Plain province and exists within the larger East Gulf Coastal Plain physiographic section (Figure 1a, Kidd & Lambeth, 1995, Osborne et al., 1989). The site is located in the Fall Line Hills district of the province, which is characterized by low-gradient sandy upland areas dissected by severely entrenched streams (Kidd & Lambeth, 1995; Fenneman, 1938). Geologically, the region is comprised of units of sedimentary origin, with approximately 1,000-foot-thick unconsolidated Mesozoic and Cenozoic sediments that overlay lower-Cretaceous and pre-Cretaceous sedimentary rocks from adjacent physiographic provinces (Davis, 1988; Osborne et al., 1988; Raymond et al., 1988). Upland areas are primarily high terrace deposits that can be as much as 100 feet thick (Kidd & Lambeth, 1995), and are underlain by the Eutaw Formation and Tuscaloosa Group geologic units (Osborne et al., 1988, 1989). This site is located in a region of outcropping of the Eutaw formation, and given that both this and the Tuscaloosa Group units are the primary water-bearing units for the region due to their highly conductive sand and gravel beds, these units can contribute water to nearby streams as upward discharge via fractures in the clay confining layers (Kidd & Lambeth, 1995). Geomorphically, the region is low- to moderate-gradient, with greater relief occurring in stream valleys (Raymond et al., 1988). The unconsolidated sediments are primarily composed of gravels, sands, silts, and clays, and result in deep, highly weathered soils with structured horizons (Alabama Cooperative Extension System, 2018; Neilson, 2007; Kidd & Lambeth, 1995). The soils are primarily well-drained ultisols with argillic confining horizons; dominant soil series include Luverne-Smithdale complexes as well as the Lucedale and Bama soil series (Soil Survey Staff, 2023). Stream sediments are primarily sand, with portions of the network eroding down to argillic confining layers. Hydrologically, the Tanglewood Biological Station drains an unnamed tributary of Fivemile Creek, which is in the larger Black Warrior River and Mobile Bay basins.

The Tanglewood Biological Station is a 560-acre nature preserve with a well-documented historical record. The majority of the property and entirety of the research watershed is forested, with upland areas dominated by loblolly pine (*Pinus taeda*) and American sweetgum (*Liquidambar styraciflua*) with a clear transition to older hardwood and riparian species in the lowland riparian areas (e.g., Florida anise, *Illicium floridanum*; American hornbeam, *Carpinus caroliniana*). The property was deeded in 1824 to the Harris family who homesteaded the land prior converting it to a small-scale plantation. The property was predominantly terraced intensive agriculture for the majority of the 19th century, and was gradually converted to forest starting circa 1870. As lumber production in the region increased around the turn of the 20th century (Fox et al., 2007), the property has been periodically harvested for silviculture. Today, the property is maintained by the University of Alabama as a nature preserve and research station.

In this region, geomorphology and climate interact to create distinctive low-gradient headwater systems. Tanglewood, like many headwater systems in the region, has highly erodible soils that interact with past agricultural land uses and high subsurface water storage capacities to form highly dendritic and dense network structures with distinct hydrogeomorphic features (Figure 2). Here, we defined hydrogeomorphic features based on distinct geomorphic characteristics such as valley shape and degree of incision that are both formed by and contribute to hydrologic patterns such as hydrologic state and water table lowering (*sensu* Cain et al., 2025).

For the purposes of this study, we identified three distinct hydrogeomorphic features in our watershed: (1) erosion-dominated incised channels (Figure 2a), (2) transport-dominated intact riparian zones (Figure 2b), and (3) deposition-dominated wetland-stream complexes (Figure 2c). These hydrogeomorphic features occurred in a predictable order across short stream distances, with incised channels occurring in high-gradient areas that flow into sections of the river corridor with intact riparian zones, and then downstream, zones with sediment deposition that form wetland-stream complexes occur at low-gradient slope breaks. Incised channels were defined here as > 0.5 m of incision between the streambed and banks. Incised channels often had relatively stable banks, with no clear evidence of bank failure throughout the study period; they often initiated at obvious channel heads that formed at knickpoints in clay soil horizons or vegetative structures. Intact riparian zones were defined here as sections of the river corridor with clear bed-and-bank structure that were incised < 0.5 m and were predominantly composed of sandy substrate with wide (approximately 20 to 30 m) riparian zones. Wetland-stream complexes were defined here as sections of the river corridor where low slope gradients created braided, multi-threaded streams between riparian wetlands and had large depositional areas for sediment and organic matter with highly organic riparian soils.

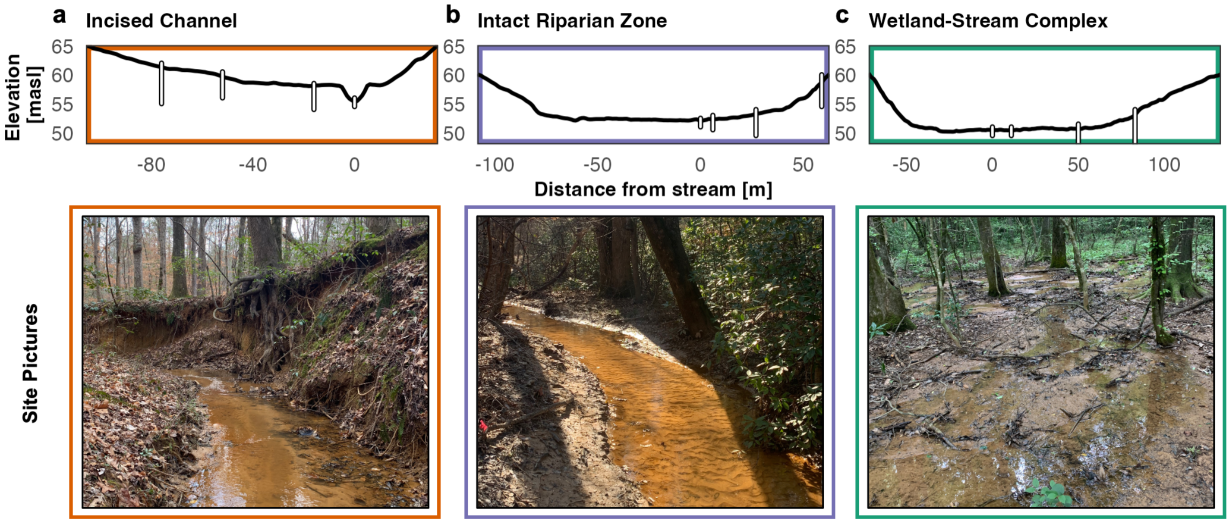

Figure 2. Valley cross-sections, well transect locations (hollow black vertical segments), and site pictures for each of the three hydrogeomorphic features in this study watershed. (**a**) The incised channel hydrogeomorphic feature, with groundwater monitoring wells within the larger valley cross-section of elevation. This 140 m cross-section shows the narrow valley bottom, as well as the distinct channel incision shown in the site picture. (**b**) The intact riparian zone hydrogeomorphic feature, with both well locations and valley cross-section. This 170 m cross-section shows the wider U-shaped valley bottom, and less-incised channel shown in the site picture. (**c**) The wetland-stream complex, with both well locations and valley cross-section. This 200 m cross-section shows the wide U-shaped and low-gradient valley bottom, while the site picture shows the complex, multi-threaded channel.

2.2 Characterizing Hydrologic Connectivity

We measured watershed-scale patterns of hydrologic connectivity with stream network ASDN surveys. We measured hydrogeomorphic feature-scale patterns of hydrologic connectivity using water table elevation gradients as a proxy for groundwater-surface water interactions. We observed patterns of hydrologic connectivity at the hillslope-scale with the presence or absence of water in nested wells. To characterize groundwater-surface water connectivity, we deployed a nested series of 14 monitoring wells instrumented with HOBO U20L-04 pressure transducers. We performed all data processing and geospatial analyses described below with R version 4.0.3

(R Core Team, 2023) using the *whitebox* (Wu & Brown, 2022), *sf* (Pebesma, 2018), and *raster* (Hijmans, 2023) packages.

2.2.1 Watershed Scale

At the watershed scale, we measured ASDN expansion and contraction using seasonal network surveys as a proxy for longitudinal connectivity (*sensu* Zimmer & McGlynn, 2018). We assigned 78 survey observation nodes throughout the geomorphic stream network (defined here as all channels at least 10 cm wide with visible banks and vegetation-free beds), placing nodes approximately 100 m apart as well as downstream of every confluence. We then visited every location in January, May, August, and November 2021 to capture conditions during each of the primary climatological seasons. At each node, we measured presence or absence of water, wetted channel width, and visually estimated the percent of surface water connectedness between nodes. We conducted these surveys in a single day at baseflow conditions (i.e., > 24 hours following a precipitation event), which we assumed to be representative of seasonal baseflow conditions. We only used 51 nodes for our network analyses, as we never observed flow at 27 of the most upstream original 78 nodes. We determined that these locations could be defined as ephemeral, and thus not representative of baseflow conditions.

We estimated the total network ASDN length for the watershed using *whitebox* (Wu & Brown, 2022). Using a 1 m resolution Digital Elevation Model (DEM; National Digital Elevation Program, 2021), we first processed the DEM to remove pits and gaps. We then generated a flow direction and flow accumulation raster, respectively (Wu & Brown, 2022). We then delineated the channel network using a flow accumulation threshold that most closely resembled seasonal survey field observations of flow (here, 13,000 1 m pixels) to calculate the maximum potential ASDN extent. Then, we calculated ASDN length for each survey as stream distance between two nodes multiplied by the percent connectedness observed per survey and aggregated to a total wetted network length.

2.2.2 Hydrogeomorphic Feature Scale

To capture patterns across hydrogeomorphic features, we delineated the hydrogeomorphic features according to channel and valley topographic metrics. We delineated hydrogeomorphic features using 20 m-long valley cross-sections centered at the thalweg and oriented orthogonal to the channel at each of the 78 ASDN nodes. We then calculated a suite of topographic metrics across those cross-sections, including average cross-sectional valley slope, bank gradient as the change in elevation in a 10 m segment across the channel, and channel width-depth ratio. Incised channel nodes were defined as cross-sections with a width-depth ratio < 15 and a maximum near-channel elevation change > 0.5 m (*sensu* Rosgen, 1994; Poesen et al., 2003). We defined wetland-stream complex nodes as cross-sections with width-depth ratios > 25 (*sensu* Rosgen, 1994). We defined intact riparian zone nodes as cross-sections falling between incised channel and wetland-stream complex criteria. We then compared our field classifications to these calculated hydrogeomorphic features, which aligned for 58% of nodes (71% of the final dataset of 51 nodes that were flowing during at least one seasonal survey). The majority (68%) of the misclassified nodes occurred upstream portions of the network, and were incised channels with narrow, constricted valleys. We updated our field classifications to match our calculated hydrogeomorphic feature categories for all subsequent analyses.

Then, to measure the hydrologic state of the stream as a proxy for lateral connectivity (*sensu* Zimmer & McGlynn, 2018), we installed one well transect in each of our delineated hydrogeomorphic features. We operationalized hydrologic state as the elevation gradient of the saturated water table that would indicate gain, loss, or equilibrium of the groundwater and surface water. We installed well transects perpendicular to the stream in locations that best reflected the local topography. Each transect consisted of one shallow (< 2 m) in-stream stilling well, one deep (> 2 m) floodplain well, one set of nested wells in the lower hillslope at the transition from riparian to upland vegetation, and one deep well in the upper hillslope (Figure S1). We hand-augered all wells to depths of refusal, and soils were characterized visually by structure, color, and texture during installation. We installed all wells such that they were screened from depths of refusal to 10 cm below the soil surface, and nested deep wells were screened from depths of refusal to the depth of the identified argillic confining horizon (B_{tgx}). We instrumented wells with unvented pressure transducers recording at synchronous 15-minute intervals from January 1 to December 31, 2021. We also installed an unvented pressure transducer above-ground within the well transect for the wetland-stream complex to record site-specific barometric pressure at the same interval. We converted gage pressure to water level (m) by correcting with barometric pressure and the specific weight of water. We converted water level for each well to water table elevation (meters above sea level, hereafter masl) using surveyed elevation data. We then divided these water elevations by linear surface distance between the wells (m) to calculate water table slope (m/m) between every set of wells, which was used to calculate hydrologic state.

2.2.3 Hillslope Scale

To characterize variability of hydrologic connectivity within hydrogeomorphic features, we used nested wells and soil characteristics to measure the ability for water to move between shallow and deeper subsurface layers. As this operationalized connectivity is a function of subsurface structure, we characterized soils using structure, color, and texture from boreholes used for well installation depths. We delineated horizon depths from the soil removed from the borehole, and which were corrected to the total depth of the borehole by multiplying horizon depth by the quotient of the measured soil profile length and the borehole depth. We then converted these horizon depths to elevations using surveyed data to be compared to water elevation data (Table S1).

We installed nested wells in locations where there were identified argillic confining layers that would impede water movement (in this case, the lower hillslope position of both the incised channel and wetland-stream complex transects). Boreholes without confining layers shallower than 4 m were considered locations of high vertical connectivity and were excluded from this analysis. We installed nested wells such that the deep well was screened from the confining layer to the depth of auger refusal, and the shallow well was screened from 10 cm below the ground surface to that confining layer (Figure S1). We instrumented these wells with pressure transducers recording at synchronous 15-minute intervals from January 1 to December 31, 2021. This resulted in the ability to detect when a perched saturated layer formed above the confining layer, as the water level in the shallow well would be closer to the surface than the water level in the deeper well. We converted water level to water elevation (masl) using surveyed elevation data, which was further aggregated to daily presence/absence of a saturated water table in each well (here, daily presence of a saturated water table required was based on a threshold of at least 12 hours).

To add further context and characterization of subsurface structure and to extrapolate soil horizons beyond the boreholes, we conducted an ERT survey including direct current and TDIP measurements on the wetland-stream complex transect (Figure 2c). We collected these data in September 2021 during dry conditions to reduce the effect of water on the measurements. We used an ABEM Terrameter LS2 system with 48 electrodes and four channels with a combination of two electrode arrays: dipole-dipole and a multichannel version of the Wenner array (following Plattner et al., 2022). The electrical current waveform consisted of a 4-s on cycle followed by a 4-s off cycle, during which measurements of the decaying electrical potential were taken at 14 timestamps, the earliest of which was after 10 ms post-current shutoff and the last after 3.4 s post-current shutoff. We used the roll-along method (*sensu* Loke et al., 2013) to extend our transect. In the riparian floodplain, the electrodes were spaced 0.5 m apart. On the hillslope, we increased the electrode spacing to 1 m.

We removed measurements for which the electrical potentials did not decay over time after current shutoff. We also removed measurements for which the apparent electrical resistivity calculated from the injected current and measured potential difference was an obvious outlier, defined as an apparent electrical resistivity less than 30 Ohm m or greater than 900 Ohm m. In total, we collected measurements for 1336 electrode combinations, of which we rejected 95. From the remaining measurements, we inverted for a resistivity profile as well as for chargeability profiles for each time step using the open-source software GIMLi (Rücker et al., 2017). From the chargeability profiles at each time step, we calculated the chargeability profile at shutoff time by fitting a time-domain Cole-Cole model (Yuval & Oldenburg, 1997) for each subsurface cell. To remove the dependence of the chargeability on the resistivity, we calculated the normalized chargeability, which is defined as the ratio between the chargeability and the resistivity, and provides a substantially improved measure for clay content (Slater & Lesmes, 2002).

3 Results

Using all our data collected across the different methods, we observed patterns in hydrologic connectivity across our three spatial scales, which will be presented here in order from the largest to smallest spatial scale. At the watershed scale, we found patterns in soils, geomorphology, and network connectivity that provided insights to finer-scale patterns we observed. At the hydrogeomorphic feature scale, we found geomorphology influenced the dynamics of groundwater-surface water connectivity. At the hillslope scale within hydrogeomorphic features, we found unique patterns in soil structure and water table dynamics.

3.1 Watershed Scale

At the watershed scale, soil and topographic characteristics interacted to create variability in channel geomorphology. Clay-rich soils were ubiquitous throughout the watershed, with 10 of the 11 boreholes containing at least one predominantly clay horizon (Table S1). Further, predominantly clay horizons made up 32.3% of all soil described across all boreholes (Table S2). Additionally, all 11 boreholes also contained at least one predominantly sand horizon, and the combination of these textures resulted in highly erodible soils both near the stream and across the hillslopes. Additionally, steep (20%) hillslopes paired with variably wide and low-gradient riparian corridors resulted in a mosaic of topographic conditions throughout the watershed (Figure 1b-d). There was a significant linear relationship between cross-sectional valley slope and distance to outlet ($p < 0.001$), with significantly steeper valley slopes in the upper reaches of the watershed that decreased closer to the watershed outlet. Further, for the 51 nodes across the watershed, the cross-sectional valley slope was significantly steeper in the incised channel hydrogeomorphic features than both the intact riparian zone and wetland-stream complex features ($p < 0.01$, Kruskal-Wallis Test; Figure S2).

In addition to the patterns in cross-sectional valley slope, we observed distinct patterns in longitudinal channel slope across our hydrogeomorphic features. Stream channel slope differed significantly across our hydrogeomorphic features ($p \ll 0.01$, Kruskal-Wallis Test; Figure 1d). Channel slope was highest in the incised channel hydrogeomorphic feature, and lowest in the wetland-stream complex hydrogeomorphic feature. This pattern in longitudinal channel slope, as well as the patterns in cross-section valley slope aligned with our field observations of riparian corridor topographic patterns across the network. The upper reaches of the watershed, where cross-sectional valley slope gradients were steepest and riparian corridors were narrow, were dominated by the incised channel hydrogeomorphic feature. Moving downstream, incised channels quickly transitioned to intact riparian zone features as both valley and channel slopes decreased. Continuing downstream, knickpoints and channel slope increases resulted in additional incised channel hydrogeomorphic features occurring in the middle reaches of the watershed before again transitioning to intact riparian zone sections following channel slope decreases. Finally, at the most downstream portion of the network where the riparian corridor was widest and valley and channel slopes were lowest, sediment deposition created wetland-stream complex features (Figure 1d).

Across the study period, hydroclimatic variability resulted in relatively minimal network expansion and contraction. The network was fully connected in February, and drying occurred in May at two nodes before completely reconnecting in August. By November, the network was dry at 6 nodes. Therefore, the proportion of wet nodes fluctuated from 100% to 88% throughout the year, with the driest period in November. However, ASDN length shows that the channel dynamics between the 51 nodes were more complex: ASDN length was highest in February at 3,700 m (100% of the potential flow network), which corresponds to the full network extent at winter baseflow. ASDN length then decreased to 3,450 m (93%) in May before increasing slightly in August (97%) and decreasing again in November to 3,520 m (95%). However, ASDN length was lowest in May, representing 93% of the total potential flow network (Table 1). While these results suggest there is variability in magnitude and longitudinal connectivity, the flowing surface network was relatively stable across the study period. We acknowledge that these patterns are likely biased by the above-average precipitation magnitude and disproportionately wet summer in 2021: 50% of the annual rainfall fell between June and September (NOAA National Centers for Environmental information, 2023), which aligned with the observed network expansion in August. All together, these patterns show that watershed-scale network dynamics reflected seasonal hydroclimatic variability, but that the network was relatively stable.

Table 1. Watershed-Scale Results Across All Four Seasonal Surveys.

Survey month	February	May	August	November
Wet nodes (count)	51	49	51	45
Wet nodes (%)	100	96	100	88
ASDN length (m)	3,700	3,450	3,580	3,520
ASDN length (%)	100	93	97	95
Outlet-connected node proportion (%)	100	94	100	78

Using the stream network survey data, we observed variation in network drying across hydrogeomorphic features. Of the seven nodes that dried during the study period, five were nodes within the incised channel hydrogeomorphic feature (17% of the 29 total incised channel nodes), compared to two intact riparian zone nodes (13% of the 16 total intact riparian zone nodes) and zero nodes within the wetland-stream complex (Figure 3). At the network scale, drying occurred unevenly across the network, resulting in both contraction and disconnection. In May, both contraction and disconnection occurred equally, and in both locations where drying occurred, the drying was focused on the incised channel. In November, contraction and disconnection also occurred equally as often; however, drying occurred in four incised channel nodes compared to two intact riparian zone nodes (Figure 3). Additionally, only one node dried more than once, indicating hysteresis in drying that may be related to the irregular distribution of hydrogeomorphic features across these nodes.

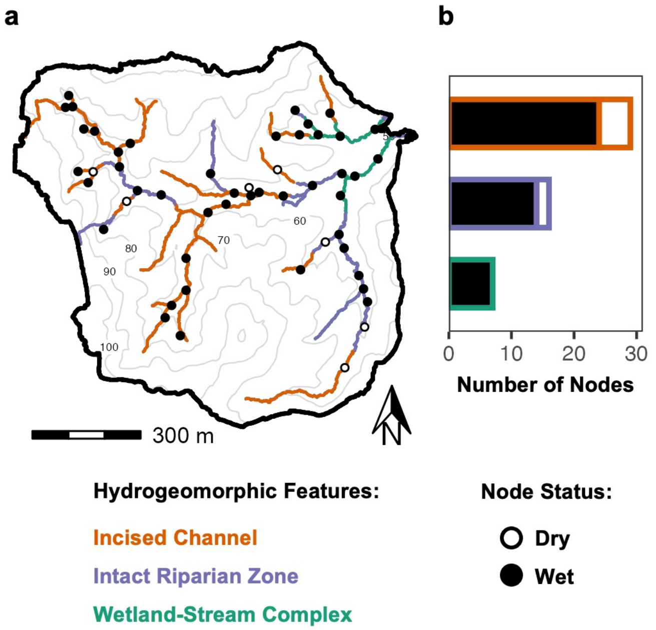

Figure 3. (**a**) A map of the study watershed, with the stream network colored by hydrogeomorphic feature, and all survey nodes marked with points (n = 51). Filled points represent locations that were wet at all survey timepoints, and points with no fill represent locations that dried at any point during the study. (**b**) A histogram of the same 51 nodes colored by hydrogeomorphic feature, indicating the distribution of nodes across the hydrogeomorphic features, as well as the proportion of wet and dry nodes for each feature. Here, the incised channel had both the largest number of total nodes (n = 29) as well as the largest number of dry nodes (n = 5). The intact riparian zone had an intermediate number of total nodes (n = 16), as well as two nodes that dried, and the wetland-stream complex had both the fewest total number of nodes (n = 7) and zero nodes that dried.

3.2 Hydrogeomorphic Feature Scale

At the scale of hydrogeomorphic features, patterns of geomorphology between the stream and riparian zone resulted in different patterns of groundwater-surface water interactions. Water table elevation (WTE) data was used to calculate hydrologic state, where elevation gradients that were higher in the groundwater well than the in-stream well indicated gaining conditions, and an elevation gradient with the in-stream well higher than the groundwater well indicated losing conditions. We found that all hydrologic states were nearly constant throughout the study period, though the magnitude and direction of this gradient varied across hydrogeomorphic features. The incised channel was gaining across the entire study period, with an average water table slope of +0.05 m/m (Figure 4a,d). The intact riparian zone was losing across the entire study period, with an average water table slope of -0.05 m/m (Figure 4b,d). The wetland-stream complex was primarily at equilibrium, though there were periods of low magnitude gain and loss that resulted in an average water table slope of +0.01 m/m (Figure 4c,d). Additionally, we found generally gaining hydraulic gradients moving towards the stream in all transects, indicating that there was potentially a gradient pushing groundwater from the hillslope towards the stream (Table 2). This is most notable in the intact riparian zone transect, where the hydraulic gradients suggest that the floodplain is both gaining with regard to the stream and the hillslope.

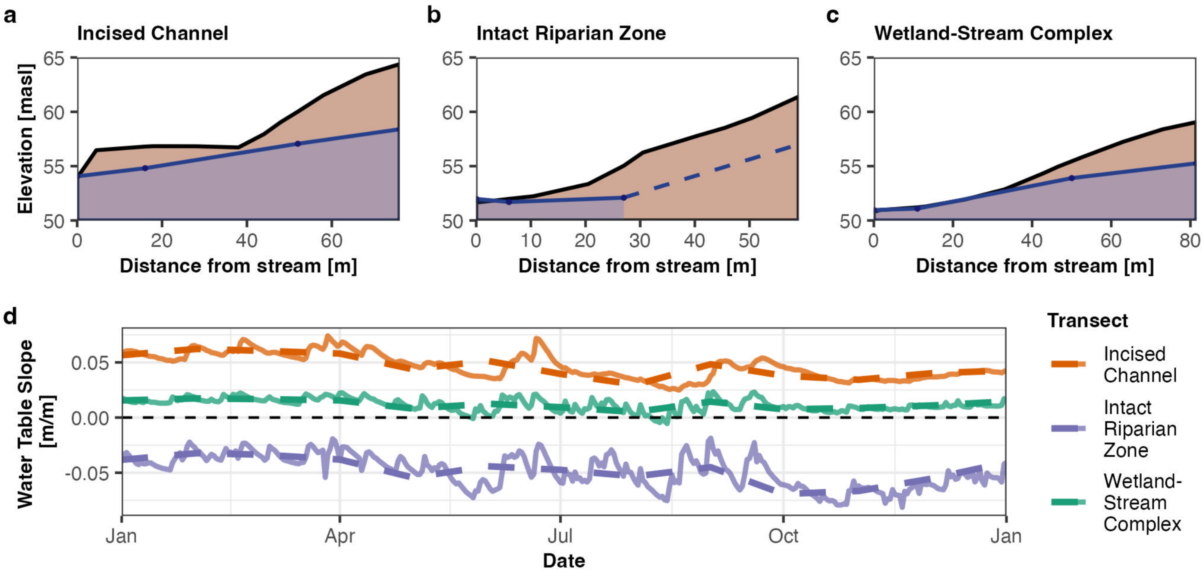

Figure 4. (**a-c**) Cross-sections of the hillslope-riparian-stream transect, with the brown polygon corresponding to the soil surface, and the blue polygon relating to the measured annual average potentiometric surface in each of the groundwater monitoring wells. Cross-section (**a**) indicated that the incised channel had a consistent head gradient towards the stream, indicating gaining conditions. Cross-section (**b**) indicated that the intact riparian zone had a head gradient towards the riparian well in both directions, indicating losing conditions in the stream, but also a potential flux of groundwater from the hillslope to the riparian zone. The dashed line indicates the highest potential gradient between the lower and upper hillslope wells, as no water was ever recorded in the upper hillslope well. Cross-section (**c**) indicated that the wetland-stream complex also had a head gradient towards the stream, suggesting gaining conditions in the channel, though at a lower

gradient. (**d**) Both the daily (line) and monthly (dashed line) hydraulic gradient between the in-stream and riparian well as Water Table Slope in each hydrogeomorphic feature. Positive water table slopes indicate flow towards the stream (gaining stream conditions).

Table 2. Hydraulic Gradients (Water Table Slope in m/m) Between All Wells Across the Hydrogeomorphic Features.

Hydrogeomorphic Feature	Stream-Riparian Gradient	Riparian-Lower Hillslope Gradient	Lower-Upper Hillslope Gradient
Incised channel	+0.05	+0.06	+0.06
Intact riparian zone	-0.05	+0.02	*NA*[a]
Wetland-stream complex	+0.01	+0.05	+0.07

Note: Positive water table slopes indicate flows towards the first location listed in each pair (e.g., towards the stream, riparian or lower hillslope location from the riparian, lower hillslope, or upper hillslope locations, respectively).

[a] Data was unavailable for the Lower-Upper Hillslope Gradient in the intact riparian zone; the upper hillslope well was only saturated during precipitation events, and so a hydraulic gradient could not be calculated.

When comparing the monthly average WTE in each well to its annual average, we found distinct patterns in variability of groundwater-surface water interactions that were not completely driven by hydroclimatic variation. The wells in the incised channel transect were the most variable across space (CV = 0.19%), showing high temporal variability in the groundwater wells but low variability in the stream channel (Figure 5b, Table S3). Conversely, all wells in the intact riparian zone transect were relatively stable (CV = 0.09%), and variability was similar between surface water and groundwater wells (Figure 5c, Table S3). In the wetland-stream complex, there was both variability throughout space and time (CV = 0.13%), but the groundwater wells were more variable than the surface water (Figure 5d, Table S3). These data show that all wells responded at different magnitudes to seasonal patterns in precipitation; all wells showed divergent responses in the incised channel regardless of water source, whereas the intact riparian zone transect showed high similarity between surface and groundwater wells, and the wetland-stream complex showed divergence between the groundwater and surface water wells, but high similarity within the groundwater wells (Figure 5).

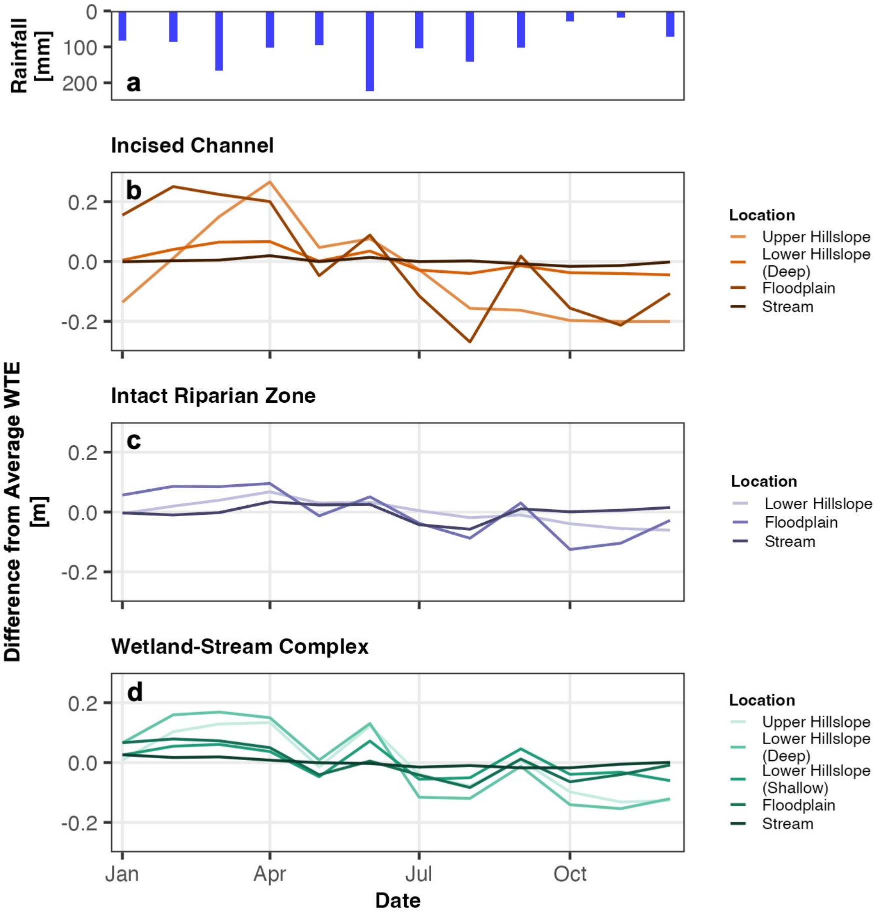

Figure 5. Difference from average WTE (calculated for each well) at monthly intervals across all three hydrogeomorphic features. Panel (**a**) shows a hyetograph of monthly precipitation (mm/month) throughout the study period. Panel (**b**) corresponds to the wells in the incised channel, which showed high variability throughout the study period in all groundwater wells. Conversely, the difference from average WTE in the stream channel was highly stable throughout time. Panel (**c**) corresponds to the wells in the intact riparian zone, which showed the least variability throughout time. All wells were similarly variable throughout time. Panel (**d**) corresponds to the wells in the wetland-stream complex, which showed moderate variability

throughout time in the groundwater wells, although all wells responded similarly. The stream well was less variable throughout time.

3.3 Hillslope Scale

At the transect scale, within-hydrogeomorphic variability was observed in the soil structure and resulting hydrologic connectivity. The borehole soils data showed that while clay-textured soils were ubiquitous throughout the watershed, argillic confining horizons were not (B_{tgx}, Table S1). Argillic confining horizons were only observed in the incised channel and wetland-stream complex transects; there were no confining horizons within 4m of the surface in the intact riparian zone transect. Additionally, we found that the argillic confining horizons were not equally distributed across each hydrogeomorphic feature – they were only observed in the lower hillslope position.

The results from the ERT/TDIP transect across the wetland-stream complex hydrogeomorphic feature showed a general pattern of highly resistive material overlaying a low resistivity substrate with the exception of a part of the hillslope, where the shallow resistive material was absent and the more electrically conductive substrate reached the surface (Figure 6a). The chargeability as well as the normalized chargeability (Figure 6b,c) was generally higher within the electrically conductive substrate compared to the chargeability of the shallow electrically resistive material. We observed a conspicuous zone of high chargeability buried at approximately 1 m depth at the upper part of the hillslope (profile position 52 m to 68 m, Figure 6b). From our ERT/TDIP results, together with soils data from our boreholes at nearby locations, we interpret that much of the hillslope was underlain by clay-rich soils. The borehole in the lower hillslope contained an argillic confining layer at approximately the same elevation as the zone of high normalized chargeability; however, the floodplain borehole did not reach deep enough to confirm the clay layer indicated by the normalized chargeability results. We note that replacing the intrinsic chargeability with the integrated chargeability, or simply with the chargeability of the first time window did not affect our results.

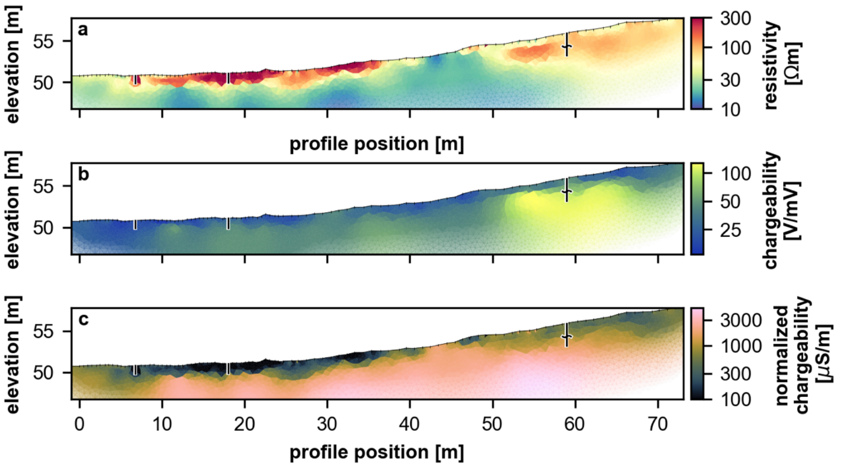

Figure 6. ERT results from the electrical resistivity and time domain induced polarization survey of the wetland-stream complex transect. The transect results for (**a**) electrical resistivity, (**b**) intrinsic chargeability, (**c**) normalized chargeability (i.e., ratio between intrinsic chargeability (b) and electrical resistivity (a)), with boreholes marked with black vertical lines indicating the elevation of the top and bottom. Additionally, the location in the lower hillslope borehole where the argillic confining horizon (B_{tgx}) was located is marked with a black ~.

Soil structure varied across hydrogeomorphic features, and resulted in a perched water table that also varied across hydrogeomorphic features and throughout time. A perched water table (defined by periods of inundation > 12 hours following a precipitation event in the shallow nested well) was observed in both sets of nested wells. Both sets of nested wells had permanent saturation with episodic precipitation event responses in the deeper well, indicating that wells were screened into the permanent water table below the confining layer (Figure 7). Additionally, both sets of nested wells showed episodic responses to precipitation events in the shallow well (Figure 7). However, the degree of permanence of water table perching was different between hydrogeomorphic features. In the incised channel transect, water table perching was only captured in response to precipitation events, which resulted in saturation for only 12% of the period of record when compared to the permanent inundation in the corresponding deep well (Figure 7b). Conversely, the wetland-stream complex transect had permanent perching in both the shallow and deep wells, indicating that there are two separate permanent water tables during the year of study – one below the confining layer, and one perched above it (Figure 7d). All together, these results suggest that subsurface heterogeneity strongly affects hydrologic connectivity, and that perched water tables vary across both space and time.

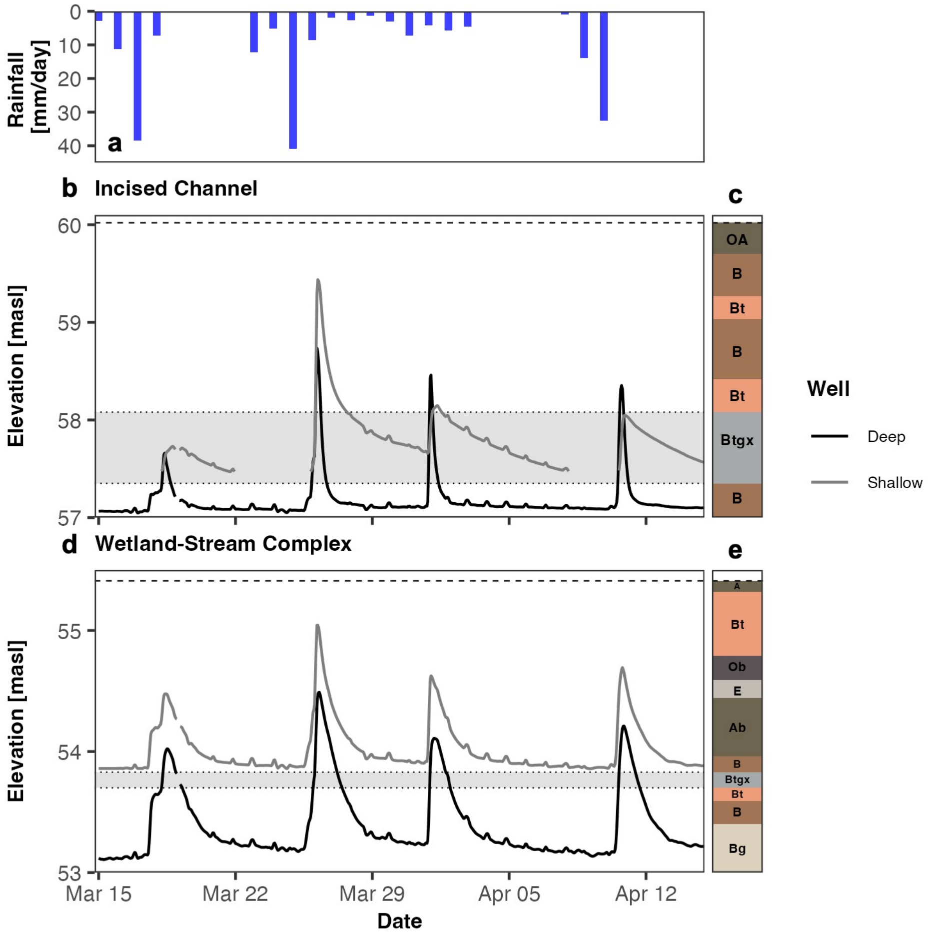

Figure 7. (**a**) A 15-day hyetograph of daily precipitation (mm/day) for the entire watershed. (**b**) 15-minute interval WTE for both nested wells in the incised channel hydrogeomorphic feature. These data suggest that there is permanent saturation below the argillic confining horizon (highlighted in grey), but only episodic perched saturation in response to storm events. Panel (**c**) shows the corresponding soil profile for the nested wells in the incised channel transect, highlighting the thick argillic confining horizon (here, B_{tgx}) near the bottom of the profile. (**d**) 15-minute interval WTE for both nested wells in the wetland-stream complex hydrogeomorphic feature (where ERT/TDIP survey was conducted, shown in Figure 6 at approximately profile position 60 m). These data suggest that there is also permanent saturation below the argillic confining horizon (highlighted in grey), but additionally, permanent saturation above it.

Therefore, these results suggest that there are two permanent water tables in this hydrogeomorphic feature. Panel (**e**) shows the corresponding soil profile for the nested wells in the wetland-stream complex, highlighting the thin B_{tgx} horizon near the middle of the profile.

4 Discussion

4.1 Hydrogeomorphic features can be used as a template for river corridor structure

Our understanding of hydrologic processes is limited by the spatial and temporal scale of our empirical measurements; hydrogeomorphic features provide an intermediate scale that can be used to better understand hydrologic connectivity and storage along the river corridor. All watersheds have some degree of heterogeneity regardless of size or location (McDonnell et al., 2007; Wainwright et al., 2022), and variability in structural landscape characteristics results in heterogeneity of hydrologic connectivity across scales ranging from soil pedons to large watersheds (McDonnell et al., 2007; Rinderer et al., 2018; Sivapalan, 2006). Feedbacks and interactions within and across scales result in emergent properties (i.e., connectivity), and therefore watershed responses are driven by processes occurring in and across hierarchical scales (McDonnell et al., 2007; Poff, 1997; Wohl et al. 2019). However, it is difficult to measure and predict heterogeneity across scales without a clear understanding of the physical processes that have created modern structural connectivity (Sivapalan, 2006; Troch et al., 2009). To aid this, many studies have suggested organizing watersheds into functional groups (McDonnell et al., 2007), geomorphic units (Schumm, 1977), and process domains (Montgomery, 1999). However, many of these characterizations have focused on larger spatial and temporal scales and do not account for hierarchical or nested scales (Wymore et al., 2023). We suggest that discretizing river corridors into smaller hydrogeomorphic features based on observable structural differences provides the opportunity to characterize the heterogeneities and processes occurring at subordinate scales. Therefore, with a better understanding of structural connectivity at finer scales, emergent properties of functional connectivity can be quantified in the larger watershed.

Here, we provide a perceptual model (*sensu* Wagener et al., 2021, McMillan et al., 2023) of the patterns of structural connectivity and its implications for storage and functional connectivity across hydrogeomorphic features in our watershed. We developed this perceptual model based on the observations and results from this study. Foundationally, all hydrologic processes within this watershed are the result of and contributors to landscape evolution across temporal scales (van der Meij et al., 2018). At the largest timescales, climate and geology interact to determine the physiographic template of the region (Miller & Robinson, 1995; Montgomery, 1999). The primary drivers of landscape evolution interact throughout time to influence topography (Montgomery, 1999; Schumm, 1977). At shorter timescales, natural disturbances (e.g., debris flows, Montgomery & Dietrich, 1994) or anthropogenic modifications (e.g., flow control structures, Wohl, 2006) further interact with the physiographic and topographic templates to determine watershed-scale patterns (van der Meij et al., 2018). Together, feedbacks between landscape drivers and changes influence the modern hydrologic, pedologic, and geomorphic conditions in a watershed, which result in patterns of structural connectivity (Larsen et al., 2012; van der Meij et al., 2018; Rinderer et al., 2018). In our study watershed, the interactions between pedologic characteristics and local slope result in three distinct hydrogeomorphic patterns occurring in a predictable cascade: erosional headwaters that flow into transport-dominated streams, which then flow into depositional wetlands (*sensu* Schumm, 1977; Frissell et al., 1986; Miller at al., 2012). In our watershed, these hydrogeomorphic features have resulted in distinct drivers of structural connectivity at the shortest timescales; we define these drivers here as stream incision, available riparian storage, and soil heterogeneity (Figure 8).

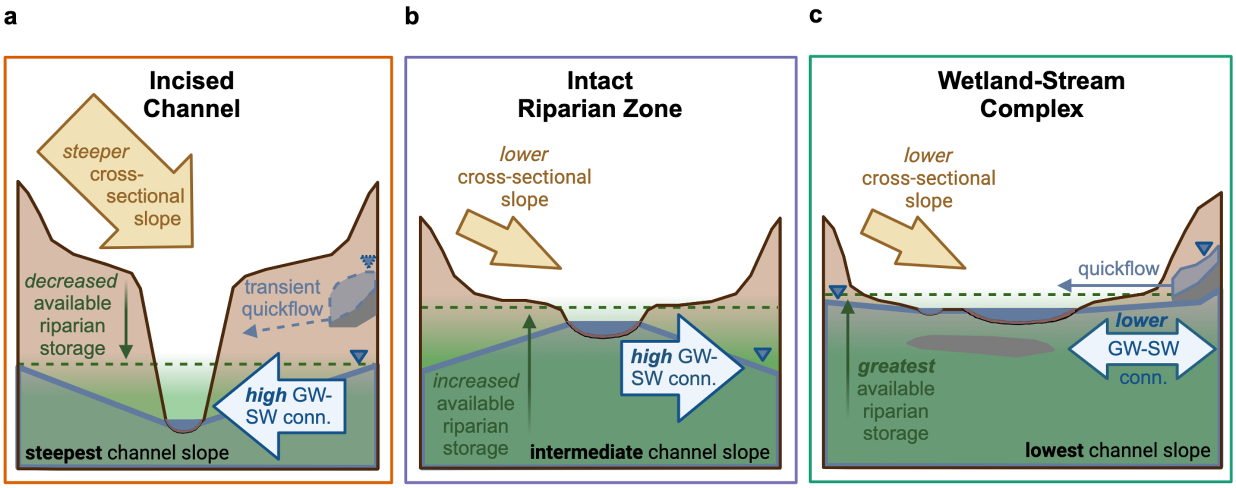

Figure 8. Our perceptual model for the primary structural and functional features of the river corridor across our hydrogeomorphic features. Panel (**a**) shows the patterns in the incised channel, where introduced incision results in decreased available riparian storage, and high

unidirectional groundwater-surface water connectivity toward the stream. The transient, perched water table is also shown on the right side of the diagram. Panel (**b**) shows the patterns in the intact riparian zone, where increased available riparian storage results in high unidirectional groundwater-surface water connectivity away from the stream. Panel (**c**) shows the patterns in the wetland-stream complex, where the greatest available riparian storage and additional floodplain wetlands result in decreased, bidirectional groundwater-surface water connectivity. The permanent, perched water table is also shown on the right side of the diagram. Created in BioRender.

Our results suggest that hydrogeomorphic features influence available riparian storage through spatial changes in both valley and channel slope as well as stream incision (Figure 8). Here, we define available riparian storage as both surface and subsurface storage pools in the near-stream river corridor (e.g., riparian soils and wetlands). Changes in storage across space (e.g., channel incision, soil structure) result in differences in functional connectivity as hydrologic state and subsequent groundwater-surface water connectivity between hydrogeomorphic features, which directly translates to either groundwater discharges to the stream (in gaining conditions) or groundwater recharge from surface water (in losing conditions) (Figure 8). Further, spatial and temporal patterns in functional connectivity can also be influenced by spatial and temporal heterogeneity in the activation of perched flowpaths. All together, these interactions of storage and connectivity across hydrogeomorphic features highlight potential sources of variability in processes along river corridors in our study watershed that drive differences in streamflow generation and source areas.

Our perceptual model of hydrologic connectivity across hydrogeomorphic features allows us to integrate all compartments of the river corridor. While other landscapes may differ in physiographic templates, land use histories, and subsequent structural connectivity, the concept of physically-based hydrogeomorphic features presented here may be applicable to other low-gradient, highly erodible landscapes. Erosive processes like incision and gully formation have been well documented, both across low-gradient systems in the southeastern USA and across the globe (Galang et al., 2007; Poesen et al., 2003; Trimble, 2008). Cascades of sediment production, transport, and deposition occur in predictable patterns across river systems due to erosion and deposition processes that are driven by topographic gradients (Montgomery, 1999;

Schumm, 1977). Gully erosion, stream incision, and other erosive processes are common in the Coastal Plain and Piedmont physiographic regions due to their highly erodible soils and land-use histories, but many other low-gradient systems are also prone to gully formation due to anthropogenic influence (Chen et al., 2020; Trimble, 2008).

Gully erosion and stream incision are both legacy effects driven by land-use changes (Galang et al., 2007; Maloney et al., 2008; Willgoose et al., 1991), and both can increase groundwater-surface water connectivity, lower water tables, and increase flashiness and aridification (Chen et al., 2020; Valentin et al., 2005; Vanmaercke et al., 2021). However, to understand how legacy effects like erosion and incision can both influence the distribution of hydrogeomorphic features and result in long-term hydrologic legacy effects, it is important to first characterize how watershed hydrogeomorphic features can influence watershed structural and functional hydrologic connectivity. Further, this is the first study to document clear differences in functional connectivity across these hydrogeomorphic features, rather than just in regions of gully formation (Chen et al., 2020). Therefore, we expect that these physically-based hydrogeomorphic features could be leveraged to better understand finer-scale patterns of groundwater-surface water interactions across watersheds and scales in low-gradient systems with land-use legacies.

4.2 Hydrologic state demonstrates the relationships between structural and functional connectivity within hydrogeomorphic features

Across hydrogeomorphic features, differences in structural connectivity defined by physical features result in distinct patterns of functional connectivity. Variability in subsurface architecture, topography, and even riparian vegetation have resulted in physical templates that influence the functional hydrologic connectivity of these regions. Incision-induced hydraulic head gradients and heterogeneities in water storage and sources can result in distinct patterns of groundwater-surface water interactions and streamflow generation that can reflect legacies of past land use.

4.2.1 Incised Channel Hydrogeomorphic Feature

Structurally, the incised channel hydrogeomorphic feature represents an erosion-dominated zone with little available riparian storage. In our study watershed, sections of the river corridor in the incised channel zone are farthest upstream in the network (Figure 1), and often initiate at obvious channel heads that formed at knickpoints in clay soil horizons or vegetative structures. Here, incised channels also correspond to upstream portions of the network with narrow, constrained valleys and steep hillslopes. These areas of incised channel features occur in the areas of both steepest cross-sectional valley and longitudinal stream channel slope (Figure 1d), which aligns with observations from other studies (e.g., Menéndez-Duarte et al., 2007; Schumm, 1977). Incision results in a decrease in the available storage of the riparian zone, either as water table lowering has decreased the soil storage that can be accessed by the stream (Figure 8a), or as constrained valleys have little to no riparian zone development. Further, in many of these incised channels, the stream has become disconnected from the riparian floodplain, meaning that there is no capacity for event-driven bidirectional flow (e.g., Squillace, 1996; Zimmer & McGlynn, 2018). Additionally, the soils in this hydrogeomorphic feature are the least organic with high clay proportions, which decreases the ability for water to move through the soil and increases preferential flow. Altogether, streams in these incised channel zones represent both the feedbacks from and causes of increased erosion due to anthropogenic impacts.

Functionally, these structural characteristics interact to create a hydrologically stable channel that was gaining across the duration of the study, meaning that there was consistent groundwater discharge into the stream channel from the nearby riparian zone (Figure 8). The observed head gradient is likely a result of the elevation gradient that stream incision introduced (Chen et al., 2020). Further, the hydrologic state results support our hydrogeomorphic perceptual model – the decreased riparian storage will result in higher groundwater discharges to the stream, and limit bidirectional flow back into the riparian groundwater (e.g., Hester et al., 2020; Hucks Sawyer et al., 2009; Zimmer & McGlynn, 2018). Our finding that surface water and groundwater responded differently to seasonal precipitation patterns further supports our perceptual model; the hydrologic gradient introduced by the steam incision and constant gaining conditions results in highly temporally stable streamflow. Further, the dissimilarity between the surface water and the groundwater well dynamics suggests a decoupling between the riparian corridor and the hillslope. While our results are limited to one above-average precipitation year, we expect that the structural connectivity of this feature generates a stable and persistent hydraulic gradient moving toward the stream across timescales; we would only expect a gradient reversal in dry conditions if the riparian water table recedes below the elevation of the streambed. All together, these results indicate that in terms of functional connectivity, streams in incised channel features are highly connected to the groundwater through unidirectional hydraulic gradients that generate stable streamflow.

4.2.2 Intact Riparian Zone Hydrogeomorphic Feature

Structurally, the intact riparian zone represents a transport-dominated feature with high available riparian storage. Streams in the intact riparian zone hydrogeomorphic feature were defined as having clear bed-and-bank structure and access to an obvious riparian zone (delineated by riparian vegetation such as Florida anise, *Illicium floridanum*) that was incised < 0.5 m. In our study watershed, these sections of the river corridor tend to occur in the middle portions of the network. Intact riparian zones are almost always downstream of incised channels, where the valley begins to widen, valley and channel slopes decrease, and channels shift from erosion-dominated to transport-dominated (*sensu* Schumm, 1977). Unlike the incised channel feature, streams in the intact riparian zone have access to their adjacent floodplains during high flows, which results in high available riparian storage as well as the opportunity for bidirectional event-driven flow and groundwater recharge (Jung et al., 2004; Zimmer & McGlynn, 2018). Further, intact riparian zones are predominantly composed of sandy substrate, and the soils in these areas are predominantly sandy clays as a result, which has a higher permeability than upstream incised channel soils.

Functionally, across the intact riparian zone we observe a hydraulic gradient from the stream to the adjacent riparian zone. This gradient suggests the stream was consistently and significantly losing during the study period, resulting in unidirectional surface water recharge to the riparian groundwater. Unlike the incised channel, we expect that the losing conditions were a direct result of the same volume of water discharging into a region of increased available riparian storage, which supports with our conceptualization of this hydrogeomorphic feature (Figure 8). This conceptualization also agrees with our findings of high similarity in water table response across all wells and greater stream variability, where consistent losing conditions results in riparian groundwater response mirroring stream conditions, and those stream conditions varying throughout time. Additionally, we would expect this pattern to persist across time-scales, given that we observed unidirectional hydraulic gradients away from the channel even in an above-average precipitation year. All together, these results indicate that in terms of functional connectivity, the intact riparian zone is highly responsive to upstream flows as well as a region of groundwater recharge.

4.2.3 Wetland-Stream Complex Hydrogeomorphic Feature

Structurally, the wetland-stream complex represents a deposition-dominated zone with high available riparian storage. Wetland-stream complexes were defined here as river corridors where the low-gradient stream threaded between riparian wetlands and were depositional areas for sediment and organic matter (Schumm, 1977). In our study watershed, the wetland-stream complex is the most downstream region of the network and occurs in wide U-shaped valleys. Like streams in the intact riparian zone, wetland-stream complexes have full access to their riparian floodplains, and in addition, have access to isolated surface-water wetlands during high flows. This access results in both high available riparian storage in both the surface and subsurface, and the potential for both lateral surface water flows and bidirectional flows during events (*sensu* Ward, 1989; Zimmer & McGlynn, 2018). Additionally, channels in this hydrogeomorphic feature have highly organic sediments, as well as highly organic riparian soils, which results in both greater hyporheic flows and subsurface permeability. Altogether, the wetland-stream complex was a hydrologically dynamic downvalley system with low gradients and high riparian available storage.

Functionally, these structural features create sections of the river corridor that are variable in flow sources and are controlled by both upstream and local conditions. The wetland-stream complex was at an equilibrium throughout the period of record: there was primarily a slightly gaining hydraulic gradient, but the wetland-stream complex was also the only feature that fluctuated between hydrologic states at any point (i.e., from gaining most days to losing others, Figure 4). Therefore, this hydrogeomorphic feature is the only one with measured bidirectional flows, which is a result of both upstream and local conditions. Further, the wetland-stream complex feature has the highest available riparian storage in surface water and groundwater pools (Figure 8c). This aligns with our findings that there was high similarity among groundwater wells, but divergence between groundwater and surface water – suggesting a decoupling of the stream from the river corridor, given that surface water is influenced by upstream conditions. Therefore, our results show that the wetland-stream complex modulates both upstream surface flows and local subsurface flows to maintain stable streamflow, which aligns with findings in other wetland-dominated areas (e.g., Bullock & Acreman, 2003; McLaughlin et al., 2014; Wegener et al., 2017). This further aligns with our network length results, where no nodes in the wetland-stream complex dried. Due to the role this hydrogeomorphic feature plays in maintaining stable streamflow, paired with observations from other studies (e.g., Fairfax & Whittle, 2020), we expect that these observed patterns in hydraulic gradients would persist even outside of high-precipitation years. All together, these results indicate that wetland-stream complexes are dynamic zones that modulate bidirectional fluxes between surface and groundwater sources.

4.3 Perched flowpath activation demonstrates spatial and temporal heterogeneity within hydrogeomorphic features

Within hydrogeomorphic features, fine-scale heterogeneity in structural connectivity drives the location and magnitude of perched flowpaths. Perched flowpaths are driven by confining layers and soil horizons with contrasting hydraulic conductivities (Baird & Low, 2022; Weyman, 1973). Activation of these perched flowpaths represents a form of quickflow (i.e., shallow subsurface flow that is routed rapidly towards the stream in response to precipitation events through matrix or preferential flow, *sensu* Carey & Woo, 2001; Scaife et al., 2020) between surface water and groundwater, and can have a variety of impacts on hydrologic connectivity across timescales. At short timescales, this quickflow can result in flashier streamflow responses to storm events, and at longer timescales, can result in decreased groundwater recharge as infiltration is routed to surface water rather than groundwater (McDaniel et al., 2008; Niswonger & Fogg, 2008; Zimmer & McGlynn, 2017). In our study, perched flow was observed to only occur in the lower hillslope position, where confining clay horizons were within 4 m of the soil surface. However, the ERT/TDIP survey demonstrated that a high normalized chargeability layer (Figure 6c), which we interpret to be a confining clay layer, was heterogeneous in depth across space, occurring at variable depths within the subsurface. Therefore, we expect that perched flow is likely distributed patchily in this watershed and does not contribute equally to streamflow in all hydrogeomorphic features nor even within any given hydrogeomorphic feature. This patchiness may affect whether perched flowpaths affect groundwater recharge and quickflow responses.

Additionally, the timing of perched flowpath activation differed across hydrogeomorphic features, which could result in variability in streamflow generation processes. As discussed, perched flow can represent a distinct source of streamflow generation, as well as variability in that source throughout time (Niswonger & Fogg, 2008; Zimmer & McGlynn, 2017). Perched flow was ephemeral in the incised channel hydrogeomorphic feature given that it was only observed 12% of the study period, and only in response to storm events and likely higher antecedent soil moisture. This likely means that in the incised channel hydrogeomorphic feature, perched flowpath activation represents quickflow, and contributions to streamflow are limited to event runoff. However, perched flow was perennial in the wetland-stream complex, which could mean that streamflow is potentially a mixture of shallow and deep groundwater depending on the distribution of confining clay horizons in the riparian zone (similar to the findings in Zimmer & McGlynn, 2018). Therefore, the timing and magnitude of perched flow contributions to streamflow likely differ through space and time, which can result in heterogeneity in streamflow response times (e.g., McDaniel et al., 2008).

Together, these results suggest that fine-scale heterogeneity in subsurface structure has implications for larger watershed processes. Emergent watershed properties have been well documented and are ubiquitous across systems regardless of watershed size (i.e., Musolff et al., 2017; Shogren et al., 2019; Jencso et al., 2009; McDonnell et al., 2007) and represent the feedbacks of processes occurring across subsequent smaller scales (Gentine et al., 2012; Laudon & Sponseller, 2018; McDonnell et al., 2007). Previous studies have shown that heterogeneity at finer scales (e.g., TTDs in individual hillslopes, Harman, 2015; soil hydraulic conductivity properties, Weyman, 1973) drive the patterns of runoff generation and hydrologic processes at coarser scales (e.g., water age distributions at watershed outlets, Harman, 2015; McGuire et al., 2005). However, it is still difficult to predict watershed-scale patterns using finer-scale heterogeneities given the existing gap between patterns and process (Jencso et al., 2009).

Therefore, we expect that incorporating hillslope and hydrogeomorphic feature processes will improve modeling of the patterns of runoff generation at the watershed scale. Here, we have made an initial attempt to describe potential heterogeneities that are likely important, despite not capturing all processes at all scales.

Further, we acknowledge that our understanding of streamflow generation in these areas is limited by our methods: our monitoring wells measured hydraulic head gradients and were unable to quantify flux, so we are unable to quantify how much of the observed perched flow is routed to streamflow. Additionally, our wells were only able to measure saturation, while some (albeit, small) portion of quickflow can also be unsaturated interflow through the soil matrix, which we are unable to account for. Despite these limitations, we anticipate that the spatial and temporal patterns of perched flowpath activation reveal the influence of subsurface heterogeneity on hillslope-scale hydrologic connectivity.

4.4 Implications

Altogether, our results suggest that hydrogeomorphic features provide an operational, intermediate scale to quantify hydrologic processes along the river corridor, and importantly, how those processes impact watershed-scale responses. Intermediate spatial scales are often the hardest to define, and multiple definitions of the intermediate scale (e.g., process domains, geomorphic units, river corridors, or valley segments; Montgomery, 1999; Schumm, 1977; Harvey & Gooseff, 2015; Wegener et al., 2017) have skewed our understanding of subsequent processes to specific locations and regions (e.g., high-gradient temperate regions; Burt & McDonnell, 2015). Further, these definitions are still immensely spatially variable, ranging from multiple stream reaches to entire basins. Therefore, we propose that using hydrogeomorphic features will further enable investigations of all compartments of the river corridor that integrate both upstream influences with adjacent lateral hydrological processes.

Further, in the context of our results at the hydrogeomorphic feature scale, there are clear implications for ecosystem functions that emerge from the observed patterns of structural and functional connectivity. Incised channels with unidirectional hydraulic gradients toward the stream have the long-term potential to lower water tables and decrease water availability for riparian vegetation (Loheide & Booth, 2011; Valentin et al., 2005; Vanmaercke et al., 2021;

King & Keim, 2019). For example, Turner et al. (2015) observed the functional composition of riparian vegetation in the Alabama Piedmont was a function of channel incision and subsequent depth to groundwater. Additionally, incised channels can decrease groundwater recharge via overbank flows (Winter, 1995; Zimmer & McGlynn, 2018), further exacerbating hydrologic droughts (*sensu* Groffman et al., 2003).

Conversely, intact riparian zones are highly dynamic portions of the stream network, and can regulate groundwater recharge and network connectivity (Jung et al., 2004; Godsey & Kirchner, 2014; Larned et al, 2011), nutrient flux and transformation (Gu et al., 2012; McClain et al., 2003; McGlynn & McDonnell, 2003), and community structure through riparian water availability and habitat complexity (Burt et al., 2002; Swanson et al., 1982; Junk et al., 1989; Tockner et al., 2000). For example, Ploum et al. (2021) found that low-gradient riparian zones contributed direct hydrologic and biogeochemical inputs to stream channels, serving as key linkages to upland environments. Further, they observed higher vegetative species diversity, with unique plant communities that facilitate biogeochemical cycling and limit decomposition within the riparian zone.

Lastly, wetland-stream complexes modulate both upstream and local signals, and their stable flows sustain key habitats (Leibowitz et al., 2018; Leigh et al., 2010), support groundwater recharge on shorter timescales (Jung et al., 2004; Ward, 1989), as well as serve as key hotspots for nutrient processing and anaerobic processes within the river corridor (Cheng & Basu, 2017; McClain et al., 2003). For example, Schulz et al. (2024) found that wide, low-gradient river corridors had high floodplain-groundwater exchange fluxes. Additionally, Wohl et al. (2018) and others found that these low-gradient depositional regions of the river corridor increase storage of organic matter (e.g., woody debris) and sediment, which creates a positive feedback and generates more system heterogeneity (Czuba & Foufoula-Georgiou, 2015). Further, these regions of the river corridor promote resilience from disturbances such as drought and wildfire (Hood and Bayley 2008, Fairfax & Whittle 2020). Taken together, hydrogeomorphic features serve as an effective means of segmenting the river corridor into functional units, providing a valuable framework for studying and managing hydrologic and ecosystem functions.

5 Conclusions

We measured hydrologic connectivity across dimensions and scales to characterize potential drivers of streamflow generation in a headwater system in the Coastal Plain physiographic province. We used hydrogeomorphic features as an intermediate spatial scale that could be used to quantify hydrologic processes across the entire river corridor. In Coastal Plain settings, headwater systems often have cascades of incised channels, intact riparian zones, and wetland-stream complexes occurring across small (< 200 m) spatial scales. When investigating representative transects within a Coastal Plain watershed, our study found distinct patterns of hydrologic connectivity across these hydrogeomorphic features, in addition to distributed patches of perched flowpaths. All together, these results show the importance of considering hydrologic fluxes across both dimensions and scales, and provide an initial characterization of streamflow generation in an understudied low-gradient region. The Coastal Plain is an expansive region in the USA, and its highly weathered and deep soils paired with humid climate and land-use legacies provide an opportunity to study potentially unique drivers of hydrologic fluxes at small scales. Given the results of this study, we suggest that further work should focus on the role of preferential flow and transient, perched flowpaths on streamflow generation, as the patchy distribution of argillic confining horizons within watersheds is likely a potential factor in the timing and magnitude of hydrologic fluxes in these watersheds. While these results are limited by the scope of one watershed during an above-average precipitation year, we believe that both hydrogeomorphic features as a scale of study and potential drivers of streamflow identified here can be used further, and further work should expand study of this intermediate scale to other Coastal Plain watersheds as well as headwater systems across diverse physiographic provinces.

Acknowledgments

The authors received support from the AIMS Project (funded by the National Science Foundation, Award Number 2019603); the FLOODPULSE Project (funded by the U.S. Department of Energy, Office of Science, Office of Biological and Environmental Research, Award Number DE-SC0023469), and the Alabama Water Institute. This study was conducted at the J. Nicholene Bishop Biological Station (also known as Tanglewood; Akron, AL), and the authors would like to thank the University of Alabama Department of Biological Sciences for their management and support of the study location. The authors would like to thank Dr.

Corianne Tatariw, Matthew Shockey, Kevin Shaw, Timothy Bushman, Vanessa Marshall, Stella Wilson, Dr. Jacob Dybiec, and many other friends and colleagues for their invaluable help with instrument installation and extensive fieldwork. We would also like to thank Dr. Adam Price, Dr. Ashleigh Kirker, Dr. Carla Atkinson, and Dr. Jon Benstead for their helpful feedback on ideas and early versions of the manuscript. We also thank the editor and anonymous reviewers for their time and effort in providing valuable feedback. The authors declare no conflicts of interest relevant to this study.

Open Research

Hydrologic sensor data is available on ESS-DIVE: https://data.ess-dive.lbl.gov/view/ess-dive-8d323d6ae87accb-20250213T152505258. Electrical Resistivity Tomography data and scripts are available here: 10.5281/zenodo.12766587 Figure 8 was created in BioRender. Peterson, D. (2025) https://BioRender.com/s42u452 All other data and programs used for this study have been cited above, and found publicly available at the locations listed in the references.

References

References

Aho, K., Derryberry, D., Godsey, S. E., Ramos, R., Warix, S. R., & Zipper, S. (2023). Communication Distance and Bayesian Inference in Non-Perennial Streams. *Water Resources Research*, *59*(11), e2023WR034513. https://doi.org/10.1029/2023WR034513

Alabama Cooperative Extension System. (2018). *Alabama Soils: Coastal Plain.* Retrieved September 27, 2023, from https://www.aces.edu/blog/topics/healthy-soils/alabama-soils-coastal-plain/

Alexander, R. B., Boyer, E. W., Smith, R. A., Schwarz, G. E., & Moore, R. B. (2007). The Role of Headwater Streams in Downstream Water Quality[1]. *JAWRA Journal of the American Water Resources Association*, *43*(1), 41–59. https://doi.org/10.1111/j.1752-1688.2007.00005.x

Allen, G. H., Pavelsky, T. M., Barefoot, E. A., Lamb, M. P., Butman, D., Tashie, A., & Gleason, C. J. (2018). Similarity of stream width distributions across headwater systems. *Nature Communications*, *9*(1), 610. https://doi.org/10.1038/s41467-018-02991-w

Baird, A. J., & Low, R. G. (2022). The water table: Its conceptual basis, its measurement and its usefulness as a hydrological variable. *Hydrological Processes*, *36*(6), e14622. https://doi.org/10.1002/hyp.14622

Botter, G., & Durighetto, N. (2020). The Stream Length Duration Curve: A Tool for Characterizing the Time Variability of the Flowing Stream Length. *Water Resources Research*, *56*(8), e2020WR027282. https://doi.org/10.1029/2020WR027282

Bracken, L. J., Wainwright, J., Ali, G.A., Tetzlaff, D., Smith, M.W., Reaney, S.M., & Roy, A.G. (2013). Concepts of hydrological connectivity: Research approaches, pathways and future agendas. *Earth-Science Reviews*, 119(1), 17-34. https://doi.org/10.1016/j.earscirev.2013.02.001

Brinkerhoff, C. B., Gleason, C. J., Kotchen, M. J., Kysar, D. A., & Raymond, P. A. (2024). Ephemeral stream water contributions to United States drainage networks. *Science, 384*(6703), 1476–1482. https://doi.org/10.1126/science.adg9430

Busch, M. H., Costigan, K. H., Fritz, K. M., Datry, T., Krabbenhoft, C. A., Hammond, J. C., et al. (2020). What's in a Name? Patterns, Trends, and Suggestions for Defining Non-Perennial Rivers and Streams. *Water, 12*(7), 1980. https://doi.org/10.3390/w12071980

Bullock, A., & Acreman, M. (2003). The role of wetlands in the hydrological cycle. *Hydrology and Earth System Sciences*, *7*(3), 358–389. https://doi.org/10.5194/hess-7-358-2003

Burt, T. P., & McDonnell, J. J. (2015). Whither field hydrology? The need for discovery science and outrageous hydrological hypotheses. *Water Resources Research*, *51*(8), 5919–5928. https://doi.org/10.1002/2014WR016839

Burt, T. P., Pinay, G., Matheson, F. E., Haycock, N. E., Butturini, A., Clement, J. C., et al. (2002). Water table fluctuations in the riparian zone: comparative results from a pan-European experiment. *Journal of Hydrology*, *265*(1), 129–148. https://doi.org/10.1016/S0022-1694(02)00102-6

Cain, M. R., Hixson, J. L., Jones, C. N., Rhoads, B. L., & Ward, A. S. (2025). Empirical Evidence of Dynamic Hydrogeomorphic Feature Inundation in a Lowland Floodplain. *Hydrological Processes, 39*(1), e70043. https://doi.org/10.1002/hyp.70043

Cardenas, M. B., Wilson, J. L., & Zlotnik, V. A. (2004). Impact of heterogeneity, bed forms, and stream curvature on subchannel hyporheic exchange. *Water Resources Research*, *40*(8). https://doi.org/10.1029/2004WR003008

Carey, S. K., & Woo, M. (2001). Slope runoff processes and flow generation in a subarctic, subalpine catchment. *Journal of Hydrology*, *253*(1), 110–129. https://doi.org/10.1016/S0022-1694(01)00478-4

Chen, X., Kumar, M., Richter, D. deB, & Mau, Y. (2020). Impact of gully incision on hillslope hydrology. *Hydrological Processes*, *34*(19), 3848–3866. https://doi.org/10.1002/hyp.13845

Cheng, F. Y., & Basu, N. B. (2017). Biogeochemical hotspots: Role of small water bodies in landscape nutrient processing. *Water Resources Research*, *53*(6), 5038–5056. https://doi.org/10.1002/2016WR020102

Costigan, K. H., Jaeger, K. L., Goss, C. W., Fritz, K. M., & Goebel, P. C. (2016). Understanding controls on flow permanence in intermittent rivers to aid ecological research: integrating meteorology, geology and land cover. *Ecohydrology*, *9*(7), 1141–1153. https://doi.org/10.1002/eco.1712

Covino, T. (2017). Hydrologic connectivity as a framework for understanding biogeochemical flux through watersheds and along fluvial networks. *Geomorphology*, *277*, 133–144. https://doi.org/10.1016/j.geomorph.2016.09.030

Czuba, J. A., & Foufoula-Georgiou, E. (2015). Dynamic connectivity in a fluvial network for identifying hotspots of geomorphic change. *Water Resources Research, 51*(3), 1401–1421. https://doi.org/10.1002/2014WR016139

Davis, L. (2007). Spatial Patterns of Geomorphic Processes in Channelized Tributary Streams. *Physical Geography, 28*(4), 301–310. https://doi.org/10.2747/0272-3646.28.4.301

Davis, M. E. (1988). *Stratigraphic and hydrogeologic framework of the Alabama Coastal Plain,* (Water-Resources Investigations Report No. 87–4112). U.S. Geological Survey. Retrieved from https://pubs.usgs.gov/publication/wri874112

Dohman, J. M., Godsey, S. E., & Hale, R. L. (2021). Three-Dimensional Subsurface Flow Path Controls on Flow Permanence. *Water Resources Research, 57*(10), e2020WR028270. https://doi.org/10.1029/2020WR028270

Downing, J. A., Cole, J. J., Duarte, C. M., Middelburg, J. J., Melack, J. M., Prairie, Y. T., et al. (2012). Global abundance and size distribution of streams and rivers. *Inland Waters*, *2*(4), 229–236. https://doi.org/10.5268/IW-2.4.502

Doyle, M., & Ensign, S. (2009). Alternative Reference Frames in River System Science. *BioScience*, *59*(6), 499–510. https://doi.org/10.1525/bio.2009.59.6.8

Dunne, T., & Black, R. D. (1970). An Experimental Investigation of Runoff Production in Permeable Soils. *Water Resources Research*, *6*(2), 478–490. https://doi.org/10.1029/WR006i002p00478

Epps, T. H., Hitchcock, D. R., Jayakaran, A. D., Loflin, D. R., Williams, T. M., & Amatya, D. M. (2013). Characterization of Storm Flow Dynamics of Headwater Streams in the South Carolina Lower Coastal Plain[1]. *JAWRA Journal of the American Water Resources Association*, *49*(1), 76–89. https://doi.org/10.1111/jawr.12000

Fairfax, E., & Whittle, A. (2020). Smokey the Beaver: beaver-dammed riparian corridors stay green during wildfire throughout the western United States. *Ecological Applications, 30*(8), e02225. https://doi.org/10.1002/eap.2225

Fenneman, N. M. (1938). Physiography of the Eastern United States (First Edition). McGraw-Hill.

Foster, D., Swanson, F., Aber, J., Burke, I., Brokaw, N., Tilman, D., & Knapp, A. (2003). The Importance of Land-Use Legacies to Ecology and Conservation. *BioScience*, *53*(1), 77–88. https://doi.org/10.1641/0006-3568(2003)053[0077:TIOLUL]2.0.CO;2

Fox, T. R., Jokela, E. J., & Allen, H. L. (2007). The Development of Pine Plantation Silviculture in the Southern United States. *Journal of Forestry, 105*(7), 337–347. https://doi.org/10.1093/jof/105.7.337

Frissell, C. A., Liss, W. J., Warren, C. E., & Hurley, M. D. (1986). A hierarchical framework for stream habitat classification: Viewing streams in a watershed context. *Environmental Management, 10(*2), 199–214. https://doi.org/10.1007/BF01867358

Galang, M. A., Markewitz, D., Morris, L. A., & Bussell, P. (2007). Land use change and gully erosion in the Piedmont region of South Carolina. *Journal of Soil and Water Conservation*, *62*(3), 122–129.

Gentine, P., Troy, T. J., Lintner, B. R., & Findell, K. L. (2012). Scaling in Surface Hydrology: Progress and Challenges. *Journal of Contemporary Water Research & Education*, *147*(1), 28–40. https://doi.org/10.1111/j.1936-704X.2012.03105.x

Godsey, S. E., & Kirchner, J. W. (2014). Dynamic, discontinuous stream networks: hydrologically driven variations in active drainage density, flowing channels and stream order. *Hydrological Processes*, *28*(23), 5791–5803. https://doi.org/10.1002/hyp.10310

Golden, H. E., Christensen, J. R., McMillan, H. K., Kelleher, C. A., Lane, C. R., Husic, A., et al. (2025). Advancing the science of headwater streamflow for global water protection. *Nature Water*, 1–11. https://doi.org/10.1038/s44221-024-00351-1

Gomi, T., Sidle, R. C., & Richardson, J. S. (2002). Understanding Processes and Downstream Linkages of Headwater Systems: Headwaters differ from downstream reaches by their close coupling to hillslope processes, more temporal and spatial variation, and their need for different means of protection from land use. *BioScience*, *52*(10), 905–916. https://doi.org/10.1641/0006-3568(2002)052[0905:UPADLO]2.0.CO;2

Grabowski, R. C., & Gurnell, A. M. (2016). Hydrogeomorphology—Ecology Interactions in River Systems. *River Research and Applications*, *32*(2), 139–141. https://doi.org/10.1002/rra.2974

Groffman, P. M., Bain, D. J., Band, L. E., Belt, K. T., Brush, G. S., Grove, J. M., et al. (2003). Down by the riverside: urban riparian ecology. *Frontiers in Ecology and the Environment, 1*(6), 315–321. https://doi.org/10.1890/1540-9295(2003)001[0315:DBTRUR]2.0.CO;2

Gu, C., Anderson, W., & Maggi, F. (2012). Riparian biogeochemical hot moments induced by stream fluctuations. *Water Resources Research*, *48*(9). https://doi.org/10.1029/2011WR011720

Hardison, E. C., O'Driscoll, M. A., DeLoatch, J. P., Howard, R. J., & Brinson, M. M. (2009). Urban Land Use, Channel Incision, and Water Table Decline Along Coastal Plain Streams, North Carolina. *JAWRA Journal of the American Water Resources Association, 45*(4), 1032–1046. https://doi.org/10.1111/j.1752-1688.2009.00345.x

Harman, C. J. (2015). Time-variable transit time distributions and transport: Theory and application to storage-dependent transport of chloride in a watershed. *Water Resources Research*, *51*(1), 1–30. https://doi.org/10.1002/2014WR015707

Harvey, J., & Gooseff, M. (2015). River corridor science: Hydrologic exchange and ecological consequences from bedforms to basins. *Water Resources Research*, *51*(9), 6893–6922. https://doi.org/10.1002/2015WR017617

Hester, E. T., McEwen, A. M., Kim, B. J., & Rost, E. A. (2020). Abundance, distribution, and geometry of naturally occurring streambank soil pipes. *Freshwater Science*, 39(4), 735-751. https://doi.org/10.1086/711655

Hewlett, J., & Hibbert, A. (1967). Factors Affecting the Response of Small Watersheds to Precipitation in Humid Areas. In *Proceedings of the International Symposium on Forest Hydrology*. Pergamon, Pennsylvania State University, NY.

Hijmans, R. (2023). raster: Geographic Data Analysis and Modeling. Retrieved from https://CRAN.R-project.org/package=raster

Hood, G. A., & Bayley, S. E. (2008). Beaver (Castor canadensis) mitigate the effects of climate on the area of open water in boreal wetlands in western Canada. *Biological Conservation, 141*(2), 556–567. https://doi.org/10.1016/j.biocon.2007.12.003

Hucks Sawyer, A., Bayani Cardenas, M., Bomar, A., & Mackey, M. (2009). Impact of dam operations on hyporheic exchange in the riparian zone of a regulated river. *Hydrological Processes*, *23*(15), 2129–2137. https://doi.org/10.1002/hyp.7324

Jackson, C. R., Bitew, M., & Du, E. (2014). When interflow also percolates: downslope travel distances and hillslope process zones. *Hydrological Processes, 28*(7), 3195–3200. https://doi.org/10.1002/hyp.10158

Jaeger, K. L., Sutfin, N. A., Tooth, S., Michaelides, K., & Singer, M. (2017). Chapter 2.1 - Geomorphology and Sediment Regimes of Intermittent Rivers and Ephemeral Streams. In T. Datry, N. Bonada, & A. Boulton (Eds.), *Intermittent Rivers and Ephemeral Streams* (pp. 21–49). Academic Press. https://doi.org/10.1016/B978-0-12-803835-2.00002-4

Jarvis, N., Koestel, J., & Larsbo, M. (2016). Understanding Preferential Flow in the Vadose Zone: Recent Advances and Future Prospects. *Vadose Zone Journal*, *15*(12), vzj2016.09.0075. https://doi.org/10.2136/vzj2016.09.0075

Jencso, K. G., McGlynn, B. L., Gooseff, M. N., Wondzell, S. M., Bencala, K. E., & Marshall, L. A. (2009). Hydrologic connectivity between landscapes and streams: Transferring reach- and plot-scale understanding to the catchment scale. *Water Resources Research*, *45*(4). https://doi.org/10.1029/2008WR007225

Jencso, K. G., & McGlynn, B. L. (2011). Hierarchical controls on runoff generation: Topographically driven hydrologic connectivity, geology, and vegetation. *Water Resources Research*, *47*(11). https://doi.org/10.1029/2011WR010666

Jones, C. N., Nelson, N. G., & Smith, L. L. (2019). Featured Collection Introduction: The Emerging Science of Aquatic System Connectivity I. *JAWRA Journal of the American Water Resources Association*, *55*(2), 287–293. https://doi.org/10.1111/1752-1688.12739

Jung, M., Burt, T. P., & Bates, P. D. (2004). Toward a conceptual model of floodplain water table response. *Water Resources Research*, *40*(12). https://doi.org/10.1029/2003WR002619

Junk, W., Bayley, P., & Sparks, R. (1989). The Flood Pulse Concept in River-Floodplain Systems. *Can. Spec. Public Fish. Aquat. Sci.* (Vol. 106).

Kidd, R. E., & Lambeth, D. S. (1995). *Hydrogeology and ground-water quality in the Black Belt area of west-central Alabama, and estimated water use for aquaculture, 1990* (Water-Resources Investigations Report No. 94–4074). Tuscaloosa, Alabama: U.S. Geological Survey. Retrieved from https://web.archive.org/web/20190501065314id_/https://pubs.usgs.gov/wri/1994/4074/report.pdf

King, S. L., & Keim, R. F. (2019). Hydrologic Modifications Challenge Bottomland Hardwood Forest Management. *Journal of Forestry, 117*(5), 504–514. https://doi.org/10.1093/jofore/fvz025

Kirker, A. N., & Toran, L. (2023). When impervious cover doesn't predict urban runoff: Lessons from distributed overland flow modeling. *Journal of Hydrology, 621,* 129539. https://doi.org/10.1016/j.jhydrol.2023.129539

Klaus, J., & Jackson, C. R. (2018). Interflow Is Not Binary: A Continuous Shallow Perched Layer Does Not Imply Continuous Connectivity. *Water Resources Research, 54*(9), 5921–5932. https://doi.org/10.1029/2018WR022920

Larned, S. T., Schmidt, J., Datry, T., Konrad, C. P., Dumas, J. K., & Diettrich, J. C. (2011). Longitudinal river ecohydrology: flow variation down the lengths of alluvial rivers. *Ecohydrology*, *4*(4), 532–548. https://doi.org/10.1002/eco.126

Larsen, L. G., Choi, J., Nungesser, M. K., & Harvey, J. W. (2012). Directional connectivity in hydrology and ecology. *Ecological Applications*, *22*(8), 2204–2220. https://doi.org/10.1890/11-1948.1

Laudon, H., & Sponseller, R. A. (2018). How landscape organization and scale shape catchment hydrology and biogeochemistry: insights from a long-term catchment study. *WIREs Water*, *5*(2), e1265. https://doi.org/10.1002/wat2.1265

Lee, E., Epstein, J. M., & Cohen, M. J. (2023). Patterns of Wetland Hydrologic Connectivity Across Coastal-Plain Wetlandscapes. *Water Resources Research*, *59*(8), e2023WR034553. https://doi.org/10.1029/2023WR034553

Leibowitz, S. G., Wigington Jr., P. J., Schofield, K. A., Alexander, L. C., Vanderhoof, M. K., & Golden, H. E. (2018). Connectivity of Streams and Wetlands to Downstream Waters: An Integrated Systems Framework. *JAWRA Journal of the American Water Resources Association*, *54*(2), 298–322. https://doi.org/10.1111/1752-1688.12631

Leigh, C., Sheldon, F., Kingsford, R. T., & Arthington, A. H. (2010). Sequential floods drive 'booms' and wetland persistence in dryland rivers: a synthesis. *Marine and Freshwater Research*, *61*(8), 896–908. https://doi.org/10.1071/MF10106

Loheide, S. P., & Booth, E. G. (2011). Effects of changing channel morphology on vegetation, groundwater, and soil moisture regimes in groundwater-dependent ecosystems. *Geomorphology*, *126*(3), 364–376. https://doi.org/10.1016/j.geomorph.2010.04.016

Loke, M. H., Chambers, J. E., Rucker, D. F., Kuras, O., & Wilkinson, P. B. (2013). Recent developments in the direct-current geoelectrical imaging method. *Journal of Applied Geophysics*, *95*, 135–156. https://doi.org/10.1016/j.jappgeo.2013.02.017

Lowe, W. H., & Likens, G. E. (2005). Moving Headwater Streams to the Head of the Class. *BioScience*, *55*(3), 196. https://doi.org/10.1641/0006-3568(2005)055[0196:MHSTTH]2.0.CO;2

Mahoney, D. T., Christensen, J. R., Golden, H. E., Lane, C. R., Evenson, G. R., White, E., et al. (2023). Dynamics of streamflow permanence in a headwater network: Insights from catchment-scale model simulations. *Journal of Hydrology, 620*, 129422. https://doi.org/10.1016/j.jhydrol.2023.129422

Maloney, K. O., Feminella, J. W., Mitchell, R. M., Miller, S. A., Mulholland, P. J., & Houser, J. N. (2008). Landuse legacies and small streams: identifying relationships between historical land use and contemporary stream conditions. *Journal of the North American Benthological Society*, *27*(2), 280–294. https://doi.org/10.1899/07-070.1

McClain, M. E., Boyer, E. W., Dent, C. L., Gergel, S. E., Grimm, N. B., Groffman, P. M., et al. (2003). Biogeochemical Hot Spots and Hot Moments at the Interface of Terrestrial and Aquatic Ecosystems. *Ecosystems*, *6*(4), 301–312. https://doi.org/10.1007/s10021-003-0161-9

McDaniel, P. A., Regan, M. P., Brooks, E., Boll, J., Barndt, S., Falen, A., et al. (2008). Linking fragipans, perched water tables, and catchment-scale hydrological processes. *CATENA*, *73*(2), 166–173. https://doi.org/10.1016/j.catena.2007.05.011

McDonnell, J. J., Sivapalan, M., Vaché, K., Dunn, S., Grant, G., Haggerty, R., et al. (2007). Moving beyond heterogeneity and process complexity: A new vision for watershed hydrology. *Water Resources Research*, *43*(7). https://doi.org/10.1029/2006WR005467

McGlynn, B. L., & McDonnell, J. J. (2003). Quantifying the relative contributions of riparian and hillslope zones to catchment runoff. *Water Resources Research*, *39*(11). https://doi.org/10.1029/2003WR002091

McGuire, K. J., Klaus, J., & Jackson, C. R. (2024). JAMES BUTTLE REVIEW: Interflow, subsurface stormflow and throughflow: A synthesis of field work and modelling. *Hydrological Processes, 38*(9), e15263. https://doi.org/10.1002/hyp.15263

McGuire, K., McDonnell, J., Weiler, M., Kendall, C., McGlynn, B., Welker, J., & Seibert, J. (2005). The role of topography on catchment-scale water residence time. *Water Resources Research*, *41*. https://doi.org/10.1029/2004WR003657

McLaughlin, D. L., Kaplan, D. A., & Cohen, M. J. (2014). A significant nexus: Geographically isolated wetlands influence landscape hydrology. *Water Resources Research*, *50*(9), 7153–7166. https://doi.org/10.1002/2013WR015002

McMillan, H., Araki, R., Gnann, S., Woods, R., & Wagener, T. (2023). How do hydrologists perceive watersheds? A survey and analysis of perceptual model figures for experimental watersheds. *Hydrological Processes*, *37*(3), e14845. https://doi.org/10.1002/hyp.14845

van der Meij, W. M., Temme, A. J. A. M., Lin, H. S., Gerke, H. H., & Sommer, M. (2018). On the role of hydrologic processes in soil and landscape evolution modeling: concepts, complications and partial solutions. *Earth-Science Reviews*, *185*, 1088–1106. https://doi.org/10.1016/j.earscirev.2018.09.001

Menéndez-Duarte, R., Marquínez, J., Fernández-Menéndez, S., & Santos, R. (2007). Incised channels and gully erosion in Northern Iberian Peninsula: Controls and geomorphic setting. *CATENA*, *71*(2), 267–278. https://doi.org/10.1016/j.catena.2007.01.002

Meyer, J. L., Strayer, D. L., Wallace, J. B., Eggert, S. L., Helfman, G. S., & Leonard, N. E. (2007). The Contribution of Headwater Streams to Biodiversity in River Networks[1]. *JAWRA Journal of the American Water Resources Association*, *43*(1), 86–103. https://doi.org/10.1111/j.1752-1688.2007.00008.x

Miller, J. R., Mackin, G., Lechler, P., Lord, M., & Lorentz, S. (2013). Influence of basin connectivity on sediment source, transport, and storage within the Mkabela Basin, South Africa. *Hydrology and Earth System Sciences, 17*(2), 761–781. https://doi.org/10.5194/hess-17-761-2013

Miller, J., & Robinson, K. G. (1995). *A regional perspective of the physiographic provinces of the southeastern United States.*

Montgomery, D. R. (1999). Process Domains and the River Continuum. *JAWRA Journal of the American Water Resources Association*, *35*(2), 397–410. https://doi.org/10.1111/j.1752-1688.1999.tb03598.x

Montgomery, D. R., & Dietrich, W. E. (1994). A physically based model for the topographic control on shallow landsliding. *Water Resources Research*, *30*(4), 1153–1171. https://doi.org/10.1029/93WR02979

Musolff, A., Fleckenstein, J. H., Rao, P. S. C., & Jawitz, J. W. (2017). Emergent archetype patterns of coupled hydrologic and biogeochemical responses in catchments. *Geophysical Research Letters*, *44*(9), 4143–4151. https://doi.org/10.1002/2017GL072630

Nadeau, T.-L., & Rains, M. C. (2007). Hydrological Connectivity Between Headwater Streams and Downstream Waters: How Science Can Inform Policy1. *JAWRA Journal of the American Water Resources Association*, *43*(1), 118–133. https://doi.org/10.1111/j.1752-1688.2007.00010.x

National Digital Elevation Program. (2021) LiDAR Elevation Dataset - Bare Earth DEM - 1 Meter (published 202106), accessed September, 2021 at https://datagateway.nrcs.usda.gov/

Neilson, M. (2007). *East Gulf Coastal Plain Physiographic Section*. Encyclopedia of Alabama. Retrieved January 19, 2022, from http://encyclopediaofalabama.org/article/h-1256

Nimmo, J. R. (2012). Preferential flow occurs in unsaturated conditions. *Hydrological Processes*, *26*(5), 786–789. https://doi.org/10.1002/hyp.8380

Niswonger, R. G., & Fogg, G. E. (2008). Influence of perched groundwater on base flow. *Water Resources Research*, *44*(3). https://doi.org/10.1029/2007WR006160

NOAA National Centers for Environmental information. (2023). *Climate at a Glance: County Time Series.* Retrieved from https://www.ncei.noaa.gov/access/monitoring/climate-at-a-glance/county/time-series

Osborne, W. E., Szabo, E. W., Copeland, C. W., & Neathery, T. L. (1988). *Geologic map of Alabama* (Special Map 220, scale 1:250,000). Geological Survey of Alabama. Retrieved from https://ngmdb.usgs.gov/Prodesc/proddesc_55859.htm

Osborne, W. E., Szabo, E. W., Copeland, C. W., & Neathery, T. L. (1989). *Geologic map of Alabama* (Special Map 221, scale 1:500,000). Geological Survey of Alabama. Retrieved from https://ngmdb.usgs.gov/Prodesc/proddesc_55860.htm

Pebesma, E. (2018). Simple Features for R: Standardized Support for Spatial Vector Data. *The R Journal.* 10(1), 439-446. https://doi.org/10.32614/RJ-2018-009

Peterson, B. J., Wollheim, W. M., Mulholland, P. J., Webster, J. R., Meyer, J. L., Tank, J. L., et al. (2001). Control of Nitrogen Export from Watersheds by Headwater Streams. *Science*. https://doi.org/10.1126/science.1056874

Plattner, A. M., Filoromo, S., & Blair, E. H. (2022). Multi-method geophysical investigation at Snow’s Bend, a Mississippian platform mound. *Archaeological Prospection*, *29*(3), 343–351. https://doi.org/10.1002/arp.1866

Ploum, S. W., Leach, J. A., Laudon, H., & Kuglerová, L. (2021). Groundwater, Soil, and Vegetation Interactions at Discrete Riparian Inflow Points (DRIPs) and Implications for Boreal Streams. *Frontiers in Water, 3*. https://doi.org/10.3389/frwa.2021.669007

Poesen, J., Nachtergaele, J., Verstraeten, G., & Valentin, C. (2003). Gully erosion and environmental change: importance and research needs. *CATENA*, *50*(2), 91–133. https://doi.org/10.1016/S0341-8162(02)00143-1

Poff, N. L. (1997). Landscape Filters and Species Traits: Towards Mechanistic Understanding and Prediction in Stream Ecology. *Journal of the North American Benthological Society*, *16*(2), 391–409. https://doi.org/10.2307/1468026

Poole, G. C. (2010). Stream hydrogeomorphology as a physical science basis for advances in stream ecology. *Journal of the North American Benthological Society*, *29*(1), 12–25. https://doi.org/10.1899/08-070.1

Prancevic, J. P., & Kirchner, J. W. (2019). Topographic Controls on the Extension and Retraction of Flowing Streams. *Geophysical Research Letters*, *46*(4), 2084–2092. https://doi.org/10.1029/2018GL081799

Pringle, C. M. (2001). Hydrologic Connectivity and the Management of Biological Reserves: A Global Perspective. *Ecological Applications*, *11*(4), 981–998. https://doi.org/10.1890/1051-0761(2001)011[0981:HCATMO]2.0.CO;2

R Core Team. (2023). R: A Language and Environment for Statistical Computing. Vienna, Austria: R Foundation for Statistical Computing. https://www.R-project.org/

Raymond, D. E., Osborne, W. E., Copeland, C. W., & Neathery, T. L. (1988). *Stratigraphy of Alabama* (Circular 140). Geological Survey of Alabama.

Richardson, J. S., & Danehy, R. J. (2007). A Synthesis of the Ecology of Headwater Streams and their Riparian Zones in Temperate Forests. *Forest Science*, *53*(2), 131–147. https://doi.org/10.1093/forestscience/53.2.131

Rinderer, M., Ali, G., & Larsen, L. G. (2018). Assessing structural, functional and effective hydrologic connectivity with brain neuroscience methods: State-of-the-art and research directions. *Earth-Science Reviews*, *178*, 29–47. https://doi.org/10.1016/j.earscirev.2018.01.009

Rücker, C., Günther, T., & Wagner, F. M. (2017). pyGIMLi: An open-source library for modelling and inversion in geophysics. *Computers & Geosciences*, *109*, 106–123. https://doi.org/10.1016/j.cageo.2017.07.011

Running, S., Mu, Q., Zhao, M., & Moreno, A. (2021). MODIS/Terra Net Evapotranspiration Gap-Filled Yearly L4 Global 500m SIN Grid V061 [Data set]. https://doi.org/10.5067/MODIS/MOD16A3GF.061

Scaife, C. I., Singh, N. K., Emanuel, R. E., Miniat, C. F., & Band, L. E. (2020). Non-linear quickflow response as indicators of runoff generation mechanisms. *Hydrological Processes*, *34*(13), 2949–2964. https://doi.org/10.1002/hyp.13780

Schumm, S. A. (1977). *The fluvial system* (3rd ed). John Wiley and Sons, Inc.

Schulz, E. Y., Morrison, R. R., Bailey, R. T., Raffae, M., Arnold, J. G., & White, M. J. (2024). River corridor beads are important areas of floodplain-groundwater exchange within the Colorado River headwaters watershed. *Hydrological Processes, 38*(9), e15282. https://doi.org/10.1002/hyp.15282

Shanafield, M., Bourke, S. A., Zimmer, M. A., & Costigan, K. H. (2021). An overview of the hydrology of non-perennial rivers and streams. *WIREs Water*, *8*(2), e1504. https://doi.org/10.1002/wat2.1504

Shogren, A. J., Zarnetske, J. P., Abbott, B. W., Iannucci, F., Frei, R. J., Griffin, N. A., & Bowden, W. B. (2019). Revealing biogeochemical signatures of Arctic landscapes with river chemistry. *Scientific Reports*, *9*(1), 12894. https://doi.org/10.1038/s41598-019-49296-6

Sidle, R. C., & Onda, Y. (2004). Hydrogeomorphology: overview of an emerging science. *Hydrological Processes*, *18*(4), 597–602. https://doi.org/10.1002/hyp.1360

Sivapalan, M. (2006). Pattern, Process and Function: Elements of a Unified Theory of Hydrology at the Catchment Scale. In *Encyclopedia of Hydrological Sciences*. John Wiley & Sons, Ltd. https://doi.org/10.1002/0470848944.hsa012

Slater, L., & Lesmes, D. P. (2002). Electrical-hydraulic relationships observed for unconsolidated sediments. *Water Resources Research*, *38*(10), 31-1-31–13. https://doi.org/10.1029/2001WR001075

Soil Survey Staff, Natural Resources Conservation Service, United States Department of Agriculture. Web Soil Survey. Accessed. June 2023. Available online https://websoilsurvey.nrcs.usda.gov/app/

Spence, C. (2010). A Paradigm Shift in Hydrology: Storage Thresholds Across Scales Influence Catchment Runoff Generation. *Geography Compass*, *4*(7), 819–833. https://doi.org/10.1111/j.1749-8198.2010.00341.x

Squillace, P. J. (1996). Observed and Simulated Movement of Bank-Storage Water. *Groundwater*, *34*(1), 121–134. https://doi.org/10.1111/j.1745-6584.1996.tb01872.x

Swanson, J., Gregory, S., Sedell, J. R., & Campbell. (1982). Land-water interactions : The riparian zone. *Analysis of Coniferous Forest Ecosystems in the Western United States*, 267–291.

Tetzlaff, D., Soulsby, C., Hrachowitz, M., & Speed, M. (2011). Relative influence of upland and lowland headwaters on the isotope hydrology and transit times of larger catchments. *Journal of Hydrology*, *400*(3), 438–447. https://doi.org/10.1016/j.jhydrol.2011.01.053

Tockner, K., Malard, F., & Ward, J. V. (2000). An extension of the flood pulse concept. *Hydrological Processes*, *14*(16–17), 2861–2883. https://doi.org/10.1002/1099-1085(200011/12)14:16/17<2861::AID-HYP124>3.0.CO;2-F

Trancoso, R., Phinn, S., McVicar, T. R., Larsen, J. R., & McAlpine, C. A. (2017). Regional variation in streamflow drivers across a continental climatic gradient. *Ecohydrology*, *10*(3), e1816. https://doi.org/10.1002/eco.1816

Trimble, S. W. (2008). *Man-Induced Soil Erosion on the Piedmont, 1700-1970* (2nd ed.). Ankeny, IA: Soil and Water Conservation Society.

Troch, P. A., Carrillo, G. A., Heidbüchel, I., Rajagopal, S., Switanek, M., Volkmann, T. H. M., & Yaeger, M. (2009). Dealing with Landscape Heterogeneity in Watershed Hydrology: A Review of Recent Progress toward New Hydrological Theory. *Geography Compass*, *3*(1), 375–392. https://doi.org/10.1111/j.1749-8198.2008.00186.x

Turner, I. P., Brantley, E. F., & Shaw, J. N. (2015). Floristic Composition of Alabama Piedmont Floodplains across a Gradient of Stream Channel Incision. *The American Midland Naturalist, 174*(2), 238–253. https://doi.org/10.1674/0003-0031-174.2.238

Valentin, C., Poesen, J., & Li, Y. (2005). Gully erosion: Impacts, factors and control. *CATENA*, *63*(2), 132–153. https://doi.org/10.1016/j.catena.2005.06.001

Vanmaercke, M., Panagos, P., Vanwalleghem, T., Hayas, A., Foerster, S., Borrelli, P., et al. (2021). Measuring, modelling and managing gully erosion at large scales: A state of the art. *Earth-Science Reviews*, *218*, 103637. https://doi.org/10.1016/j.earscirev.2021.103637

Vannote, R. L., Minshall, G. W., Cummins, K. W., Sedell, J. R., & Cushing, C. E. (1980). The River Continuum Concept. *Canadian Journal of Fisheries and Aquatic Sciences*, *37*(1), 130–137. https://doi.org/10.1139/f80-017

Wainwright, H. M., Uhlemann, S., Franklin, M., Falco, N., Bouskill, N. J., Newcomer, M. E., et al. (2022). Watershed zonation through hillslope clustering for tractably quantifying above- and below-ground watershed heterogeneity and functions. *Hydrology and Earth System Sciences*, *26*(2), 429–444. https://doi.org/10.5194/hess-26-429-2022

Ward, J. V. (1989). The Four-Dimensional Nature of Lotic Ecosystems. *Journal of the North American Benthological Society*, *8*(1), 2–8. https://doi.org/10.2307/1467397

Warix, S. R., Navarre-Sitchler, A., Manning, A. H., & Singha, K. (2023). Local Topography and Streambed Hydraulic Conductivity Influence Riparian Groundwater Age and Groundwater-Surface Water Connection. *Water Resources Research*, *59*(9), e2023WR035044. https://doi.org/10.1029/2023WR035044

Wegener, P., Covino, T., & Wohl, E. (2017). Beaver-mediated lateral hydrologic connectivity, fluvial carbon and nutrient flux, and aquatic ecosystem metabolism. *Water Resources Research*, *53*(6), 4606–4623. https://doi.org/10.1002/2016WR019790

Weyman, D. R. (1973). Measurements of the downslope flow of water in a soil. *Journal of Hydrology*, *20*(3), 267–288. https://doi.org/10.1016/0022-1694(73)90065-6

Willgoose, G., Bras, R. L., & Rodriguez-Iturbe, I. (1991). A coupled channel network growth and hillslope evolution model: 1. Theory. *Water Resources Research*, *27*(7), 1671–1684. https://doi.org/10.1029/91WR00935

Winter, T. C. (1995). Recent advances in understanding the interaction of groundwater and surface water. *Reviews of Geophysics*, *33*(S2), 985–994. https://doi.org/10.1029/95RG00115

Winter, T. C. (1999). *Ground Water and Surface Water: A Single Resource*. DIANE Publishing.

Wohl, E. (2006). Human impacts to mountain streams. *Geomorphology*, *79*(3–4), 217–248. https://doi.org/10.1016/j.geomorph.2006.06.020

Wohl, E., Brierley, G., Cadol, D., Coulthard, T. J., Covino, T., Fryirs, K. A., et al. (2019). Connectivity as an emergent property of geomorphic systems. *Earth Surface Processes and Landforms*, *44*(1), 4–26. https://doi.org/10.1002/esp.4434

Wohl, E., Lininger, K. B., & Scott, D. N. (2018). River beads as a conceptual framework for building carbon storage and resilience to extreme climate events into river management. *Biogeochemistry, 141*(3), 365–383. https://doi.org/10.1007/s10533-017-0397-7

Wu, Q., & Brown, A. (2022). whitebox: "WhiteboxTools" R Frontend. R package version 2.2.0. Retrieved from https://CRAN.R-project.org/package=whitebox

Wymore, A. S., Ward, A. S., Wohl, E., & Harvey, J. W. (2023). Viewing river corridors through the lens of critical zone science. *Frontiers in Water*, *5*. https://doi.org/10.3389/frwa.2023.1147561

Yuval & Oldenburg, D. W. (1997) Computation of Cole-Cole parameters from IP data. *Geophysics*, 62 (2) 436-448. doi:10.1190/1.1444154

Zanetti, F., Botter, G., & Camporese, M. (2024). Stream Network Dynamics of Non-Perennial Rivers: Insights From Integrated Surface-Subsurface Hydrological Modeling of Two Virtual Catchments. *Water Resources Research, 60*(2), e2023WR035631. https://doi.org/10.1029/2023WR035631

Zimmer, M. A., & McGlynn, B. L. (2017). Ephemeral and intermittent runoff generation processes in a low relief, highly weathered catchment. *Water Resources Research*, *53*(8), 7055–7077. https://doi.org/10.1002/2016WR019742

Zimmer, M. A., & McGlynn, B. L. (2018). Lateral, Vertical, and Longitudinal Source Area Connectivity Drive Runoff and Carbon Export Across Watershed Scales. *Water Resources Research*, *54*(3), 1576–1598. https://doi.org/10.1002/2017WR021718

AGU PUBLICATIONS

Water Resources Research

Supporting Information for

Using Hydrogeomorphic Features to Quantify Structural and Functional Hydrologic Connectivity in a Coastal Plain Headwater Stream

Delaney M. Peterson[1], C. Nathan Jones[1], Alain M. Plattner[2], Arial J. Shogren[1], and Sarah E. Godsey[3]

[1]Department of Biological Sciences, University of Alabama, Tuscaloosa, AL, USA.

[2]Department of Geological Sciences, University of Alabama, Tuscaloosa, AL, USA.

[3]Department of Geosciences, Idaho State University, Pocatello, ID, USA.

Contents of this file

Text S1
Figure S1 to S2
Tables S1 to S3

Introduction

The following contains more detailed information about the study site (i.e., location; Text S1), study design (Figure S1), and additional data. The additional data include more detailed information about the watershed-scale feature delineations (Figure S2), soils described for the project, as well as where key horizons are located (Table S1). Additionally, it contains summary statistics of both the soils data (Table S2) and water table elevation data (Table S3) used in the manuscript. All elevation data was derived from field measurements and manually surveyed relative elevation. Soil horizon elevations were corrected by multiplying the measured horizon depth by the quotient of the measured total soil profile and the measured borehole depth.

Text S1.

The study watershed is a 0.9 km^2 forested site in Hale County, Alabama (USA). The watershed outlet is located at (32.851436, -87.663652), and drains a portion of the larger Tanglewood Biological Station before flowing into Fivemile Creek.

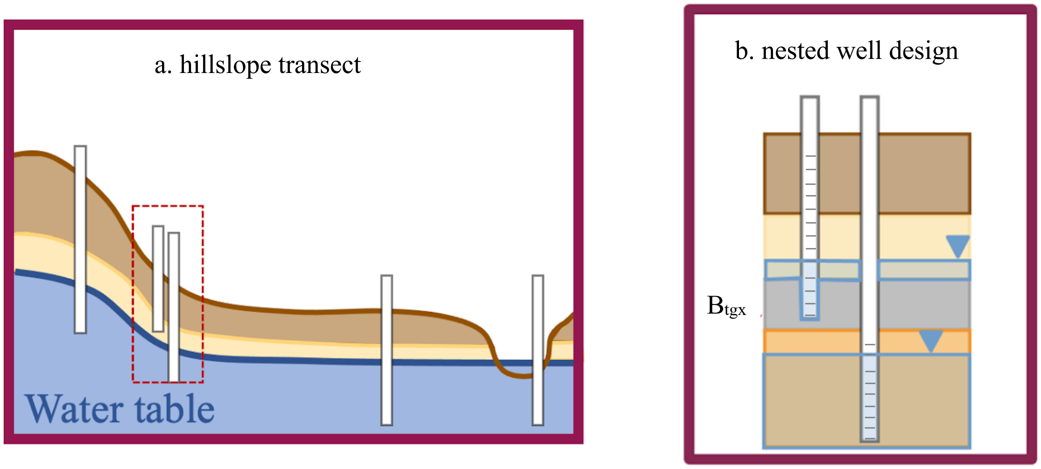

Figure S1. Site design for well installation. (**a**) shows the hillslope transect that was installed into each hydrogeomorphic feature, with one stream, one floodplain, a nested lower hillslope (indicated by the red dashed line), and one upper hillslope well. (**b**) shows the more detailed nested well design, with a shallow well screened from the argillic confining horizon (here, B$_{tgx}$) to within 10 cm of the ground surface. The deep well is screened from the bottom of the B$_{tgx}$ to depths of refusal. Both the permanent deep and perched shallow water table are indicated in blue, showing that water level is higher in the shallow well (which reflects the discontinuous perched nature of the two zones of saturation).

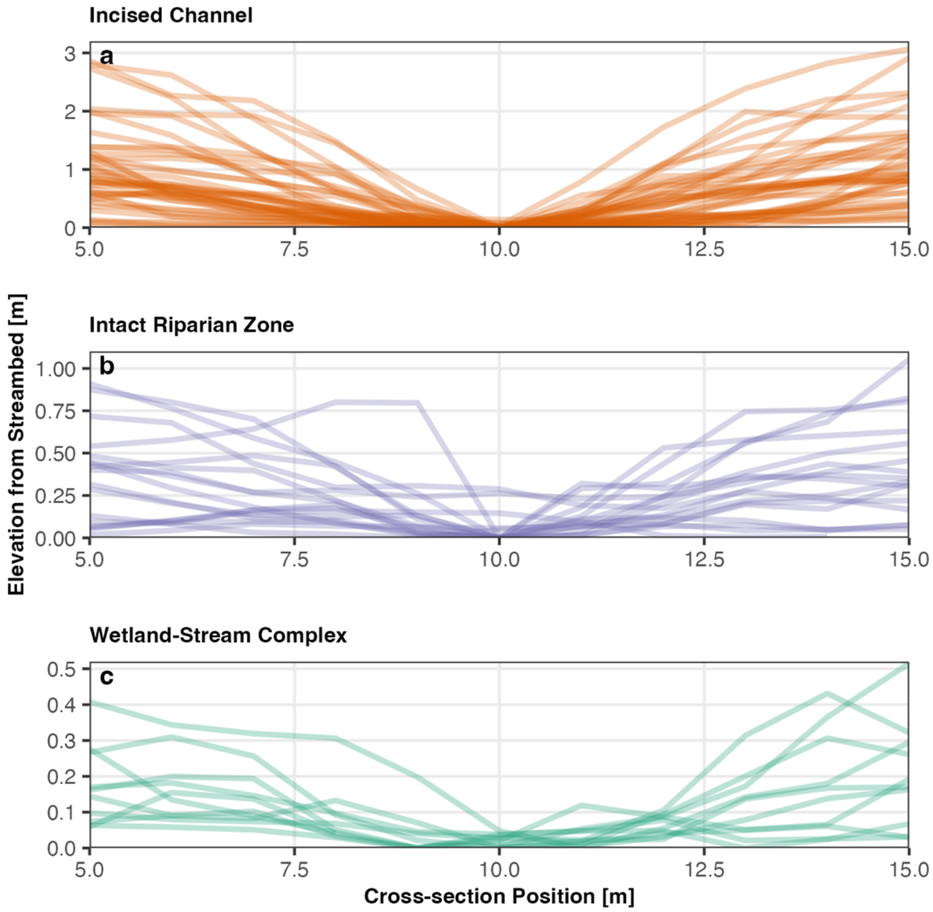

Figure S2. Cross-sections of the full set of 78 observation nodes across the network showing near-stream elevation profiles, grouped by hydrogeomorphic feature. (**a**) The incised channel feature, showing the highest proportion of cross-sections, as well as variability in the profiles. However, all cross-sections in this feature have > 0.5 m of elevation change between the stream channel (10 m Cross-Section Position). (**b**) The intact riparian zone feature, showing less change in elevation in the cross-sections, but still obvious bank profiles. (**c**) The wetland-stream complex feature, showing the lowest proportion of cross-sections and the overall lowest change in elevation across the cross-section. Further, channel profiles are generally wider between the banks, showcasing the higher width-depth ratios. Please note the variation in axis ranges across the hydrogeomorphic features.

Table S1. Soils data from all boreholes.

Hydrogeomorphic Feature	Position	Horizon	Horizon Elevation (masl)	Horizon Depth (cm)
Incised	Upper Hillslope	A	64.40	8.9
		AB	64.31	9.4
		Bt1	64.22	31.9
		Bt2	63.90	85.0
		B1	63.05	28.9
		B2	62.76	12.4
		Bt3	62.64	97.4
		B3	61.66	10.0
		Bt4	61.56	43.1
		B4	61.13	32.5
		Bt5	60.81	20.7
		B5	60.60	115.7
		B6	59.44	20.1
		Bg1	59.24	14.8
		Bg2	59.10	18.9
		B7	58.91	20.7
		Bg3	58.70	23.6
		B8	58.46	15.9
		B9	58.30	10.6
		Bt6	58.20	8.9
	Lower Hillslope (Deep)	OA	59.97	5.5
		A	59.92	11.6
		AB	59.80	15.0

		B1	59.65	28.0
		B2	59.37	15.0
		Bt1	59.22	23.9
		B3	58.98	16.4
		B4	58.82	24.6
		B5	58.57	20.5
		Bt2	58.37	34.1
		Btgx1	58.02	38.2
		Btgx2	57.64	34.8
		Bt3	57.29	17.7
		B6	57.12	21.8
		Cg1	56.90	20.5
		Cg2	56.69	43.7
		Cg3	56.26	10.9
	Lower Hillslope (Shallow)	OA	59.97	5.5
		A	59.92	11.6
		AB	59.80	15.0
		B1	59.65	28.0
		B2	59.37	15.0
		Bt1	59.22	23.9
		B3	58.98	16.4
		B4	58.82	24.6
		B5	58.57	20.5
		Bt2	58.37	34.1
		Btgx1	58.02	38.2

		Btgx2	57.64	33.3
	Floodplain	A	56.80	4.0
		AB	56.76	7.2
		BE	56.69	18.3
		E	56.51	27.9
		Eg	56.23	51.8
		B	55.71	33.4
		Bg1	55.37	43.8
		Bg2	54.94	103.5
		Bt	53.90	19.1
		Btg1	53.71	22.3
		Btg2	53.49	17.5
		Btg3	53.31	34.2
Stream	Upper Hillslope	A	61.40	17.4
		Bt	61.23	37.0
		B1	60.86	65.0
		B2	60.21	57.5
		B3	59.63	34.0
		B4	59.29	15.9
		B5	59.13	34.0
		E	58.79	37.0
		EB	58.42	59.0
		B6	57.83	24.2
		Ob	57.59	6.0
		B7	57.53	23.4

		B8	57.29	15.1
		Btgx	57.14	14.4
	Lower Hillslope	A	55.00	5.9
		Bt1	54.94	61.9
		Bt2	54.32	18.4
		Bt3	54.14	39.8
		B1	53.74	53.0
		B2	53.21	24.3
		BE	52.97	49.4
		B4	52.47	39.0
		B5	52.08	50.8
		Bg	51.57	43.5
	Floodplain	A	51.99	5.8
		AB	51.93	8.1
		Bt1	51.85	23.8
		Bt2	51.61	40.0
		Bt3	51.21	59.2
		Bt4	50.62	8.1
Wetland	Upper Hillslope	A	59.10	16.0
		Bt	58.94	58.8
		B1	58.35	145.2
		B2	56.90	64.1
		B3	56.26	60.6
		B4	55.65	81.1
		B5	54.84	45.4

		BAb	54.39	74.8
		Ab	53.64	18.7
		B6	53.45	76.6
		Bg1	52.69	13.4
		Bg2	52.55	23.2
		Btg	52.32	7.1
	Lower Hillslope (Deep)	A	55.40	9.4
		Bt1	55.31	37.6
		BtO	54.93	15.2
		Ob	54.78	20.3
		E	54.58	14.5
		Ab	54.43	21.0
		AOb	54.22	11.6
		Ab2	54.10	15.9
		B1	53.95	12.3
		Btgx	53.82	13.0
		Bt2	53.69	10.9
		B2	53.58	19.5
		Bg1	53.39	24.6
		Bg2	53.14	15.9
		Cg	52.98	25.3
	Lower Hillslope (Shallow)	A	55.40	6.3
		Bt	55.34	46.8
		BOb	54.87	11.9
		Ob	54.75	25.4

		B1	54.50	70.6
		B2	53.79	34.9
		Btgx	53.44	3.2
	Floodplain	AO	51.20	14.3
		A	51.06	17.1
		AB	50.89	13.3
		B1	50.75	23.8
		BA	50.52	28.5
		B2	50.23	17.1

Note: Each borehole contains all delineated horizons and their corresponding elevations (at the top of the horizon, masl) and depths (i.e., thickness, cm). Nested wells have the same horizons from the surface to the argillic confining horizon (here, B_{tgx}), and then the deep well includes the soil horizons below.

Table S2. Soils summary information.

Hydrogeomorphic Feature	Position	Total Depth (m)	Percent Clay Horizon	Argillic Confining Horizon
Incised Channel	Upper Hillslope	6.29	45.6%	No
	Lower Hillslope (Deep)	3.82	38.9%	Yes
	Lower Hillslope (Shallow)	2.66	48.7%	Yes[a]
	Floodplain	3.83	24.3%	No
Intact Riparian Zone	Upper Hillslope	4.40	11.7%	Yes[a]
	Lower Hillslope	3.86	31.1%	No
	Floodplain	1.45	90.7%	No
Wetland-Stream Complex	Upper Hillslope	6.85	9.6%	No
	Lower Hillslope (Deep)	2.67	30.0%	Yes
	Lower Hillslope (Shallow)	1.99	25.1%	Yes[a]
	Floodplain	1.14	0%	No

Note: Each borehole has an associated total depth (measured from the borehole, not from soils), the percentage of clay-dominated horizons, and whether there was an argillic confining horizon (here, B_{tgx}) present in the borehole.

[a] well was screened above and into (> 10 cm) B_{tgx} horizon

Table S3. Water Table Elevation (WTE) summary statistics.

Hydrogeomorphic Feature	Position	Mean WTE (m)	SD WTE (m)	CV (%)
Incised Channel	Upper Hillslope	58.4	0.156	0.27
	Lower Hillslope (Shallow)	57.7	0.144	0.25
	Lower Hillslope (Deep)	57.1	0.042	0.07
	Floodplain	54.8	0.179	0.33
	Stream	54.1	0.010	0.02
Intact Riparian Zone	Upper Hillslope	57.1[a]	0.009[a]	0.02[a]
	Lower Hillslope	52.1	0.040	0.08
	Floodplain	51.7	0.078	0.15
	Stream	52.0	0.027	0.05
Wetland	Upper Hillslope	55.3	0.101	0.18
	Lower Hillslope (Shallow)	53.9	0.052	0.10
	Lower Hillslope (Deep)	53.1	0.129	0.24
	Floodplain	51.1	0.056	0.11
	Stream	51.0	0.015	0.03

Note: Each water monitoring well has a corresponding mean annual WTE (masl), as well as the standard deviation and coefficient of variation (CV).

[a] Data for the Upper Hillslope well in the intact riparian zone was limited to immediately following precipitation events, and therefore is contained here, but excluded from the final analyses